Bioorganic Chemistry 110 (2021) 104750

Contents lists available at ScienceDirect

Bioorganic Chemistry

journal homepage: www.elsevier.com/locate/bioorg

Chromone derivatives bearing pyridinium moiety as multi-target-directed ligands against Alzheimer's disease

Shahin Abdpour [a], Leili Jalili-Baleh [b], Hamid Nadri [c], Hamid Forootanfar [d], Syed Nasir Abbas Bukhari [e], Ali Ramazani [a], Seyed Esmaeil Sadat Ebrahimi [f], Alireza Foroumadi [f], Mehdi Khoobi [f,g,*]

[a] Department of Chemistry, University of Zanjan, Zanjan, Iran
[b] The Institute of Pharmaceutical Sciences (TIPS), Tehran University of Medical Sciences, Tehran 1417614411, Iran
[c] Faculty of Pharmacy and Pharmaceutical Sciences Research Center, Shahid Sadoughi University of Medical Sciences, Yazd, Iran
[d] Department of Pharmaceutical Biotechnology, Faculty of Pharmacy, Kerman University of Medical Sciences, Kerman, Iran
[e] Department of Pharmaceutical Chemistry, College of Pharmacy, Jouf University, Aljouf, Sakaka 2014, Saudi Arabia
[f] Department of Medicinal Chemistry, Faculty of Pharmacy, Tehran University of Medical Sciences, Tehran 14176, Iran
[g] Biomaterials Group, Pharmaceutical Sciences Research Center, The Institute of Pharmaceutical Sciences (TIPS), Tehran University of Medical Sciences, Tehran 1417614411, Iran

ARTICLE INFO

Keywords:
Alzheimer's disease
Cholinesterase inhibitors
Neuroprotective activity
Anti-amyloid aggregation
Chromone
Pyridinium salts

ABSTRACT

A new serise of 7-hydroxy-chromone derivatives bearing pyridine moiety were synthesized, and evaluated as multifunctional agents against Alzheimer's disease (AD). Most of the compounds were good AChE inhibitors (IC_{50} = 9.8–0.71 μM) and showed remarkable BuChE inhibition activity (IC_{50} = 1.9–0.006 μM) compared with donepezil as the standard drug (IC_{50} = 0.023 and 3.4 μM). Compounds **14** and **10** showed the best inhibitory activity toward AChE (IC_{50} = 0.71 μM) and BuChE (IC_{50} = 0.006 μM), respectively. The ligand–protein docking simulations and kinetic studies revealed that compound **14** and **10** could bind effectively to the peripheral anionic binding site (PAS) of the AChE and BuChE through mixed-type inhibition. In addition, the most potent compounds showed acceptable neuroprotective activity on H_2O_2- and Aβ-induced .neurotoxicity in PC12 cells, more than standard drugs. The compounds could block effectively self- and AChE-induced Aβ aggregation. All the results suggest that compounds **14** and **10** could be considered as promising multi-target-directed ligands against AD.

1. Introduction

Alzheimer's disease (AD) is the most common cause of dementia and one of the major causes of mortality in the world. It is one of the most commonly debilitating disabilities in the elderly. The disease is pathophysiology associated with the decline in the level of cholinergic neurotransmitters, abnormal formation of amyloid-beta (Aβ) protein plaques and neurofibrillary collapse, appearance of hyperphosphorylated τ-protein aggregation, dyshomeostasis of biometals, oxidative stress, and neuroinflammation [1,2].

There are two forms of cholinesterase in the brain of mammals namely acetylcholinesterase (AChE) and butyrylcholinesterase (BuChE). The two forms are different genetically, structurally and in their kinetics. BuChE is found in neurons and glial cells as well as in senile plaques and tangles which is hallmarks in patients with AD. While the activity of AChE declines in the hippocampus, BuChE activity tends to increase. Recently, several evidences have been emerged indicating that BuChE plays a pivotal role in regulating the ACh level of brain in the late stage of AD. The AChE level in the brain decreases to 55–67% of normal values, while BuChE increases to 165% of the normal levels [3–5]. Moreover, AChE knockout mice models showed that BuChE can possibly substitute for AChE, to destroy ACh in synaptic cleft [6]. In addition, BuChE inhibition does not lead to peripheral adverse effects [7]. Therefore, development of highly potent and selective BChE inhibitors with the ability to reinstate ACh levels in the brain and reduced peripheral side effects, has gained much interest [8]. Furthermore, many studies have shown that both AChE and BuChE facilitate amyloid fibril formation resulting in the formation of more toxic ChE-Aβ complexes

* Corresponding author at: The Institute of Pharmaceutical Sciences (TIPS), Tehran University of Medical Sciences, Tehran 1417614411, Iran.
E-mail address: m-khoobi@tums.ac.ir (M. Khoobi).

https://doi.org/10.1016/j.bioorg.2021.104750
Received 24 August 2020; Received in revised form 16 January 2021; Accepted 13 February 2021
Available online 19 February 2021

[9,10]. Some studies have suggested that AChE forms a complex with Aβ through the hydrophobic pocket near of peripheral anionic binding site (PAS) promoting amyloid fibril formation [11]. Therefore, compounds with the ability to inhibit PAS of the enzyme, not only block ACh entrance into the catalytic core, but also inhibit the PAS-induced Aβ oligomerization [12]. *In vivo* studies also revealed that Aβ plaques accumulation in the brain tissue is associated with BuChE activity [13–15].

There are tangible shreds of evidence that toxic effect of the Aβ plaques has great role in the disease initiation and progression [16]. It has been revealed that during Aβ aggregation, accumulation of intracellular hydrogen peroxide (H_2O_2) leads to the peroxidation of lipid membrane of neurons and ultimately to the cell death [17–19]. Therefore, neuroprotection against Aβ-induced oxidative stress as a key item in the progression of the disease is recommended to combat against AD [20]. During the past decades, valuable efforts have been devoted to discovering disease-modifying drugs controlling the progression of AD, mainly focused on Aβ peptide, as a widely accepted key problem of AD. Notwithstanding all attempts, no drug candidates have been approved in advanced clinical trials since the launching of Memantine, so far.

In modern medicinal chemistry, the multi-target-directed ligand (MTDL) strategy is a well-established theory for the design and discovery of the multifunctional compounds modulating various receptors or targeting diverse enzymes to employ for the potential treatment of complex disorder like AD [21]. Multi-factorial cause of AD requires a multi-target approach for the treatment which could be achieved through the combination of effective pharmacophoric groups in a unique small molecule. This paradigm is more effective than the one-target, one-drug concept [22,23]. Drug-combination therapies for the treatment of AD lead to more beneficial therapeutic effects and result in superior *in vivo* outcomes compared to the one-target compounds having high affinity, even if the multi-target small molecules have mild activity against one or several targets [24].

Chromones with γ-benzopyrone ring are an advantageous framework for drug discovery in medicinal chemistry especially for the treatment of AD [25]. The core fragment of various flavonoids have the chromone skeleton representing a wide range of pharmacological activities, including their ability to inhibit cholinesterase enzymes [26,27], anti-Aβ aggregating property [28,29], neuroprotective [30,31], free radicals scavenging, metal ions chelating [32–34], and anti-inflammatory activities [35]. Based on MTDLs strategy, some chromone-based compounds have been evaluated against AD exhibiting valuable biological activities [36]. Recent study has indicated that chromone-2-carboxamido-alkylbenzylamine derivatives (Fig. 1) are interesting inhibitors of AChE/BuChE and Aβ aggregation, with acceptable antioxidant, and metal chelation activities [37]. The study revealed that the chromone part has great role in antioxidant and neuroprotection activity as well as anti-Aβ aggregation potency of the target compounds (Fig. 1) [37,38]. Moreover, pyridinium salt is a well-known pharmacophore having strong binding affinity towards catalytic active site (CAS) of AChE through π-stacking and charge interactions and various MTDLs bearing this moiety have been introduced so far (Fig. 1) [39,40].

Considering these findings, and in continuation of our interest in developing potent MTDLs against AD [41,42], we designed, synthesized, and evaluated biological activity of a series of novel chromone-based derivatives bearing pyridinium moiety as multi-targeted inhibitors of ChEs. We aimed to improve the inhibitory activity of the chromone scaffold against AChE and BuChE as well as AChE-induced Aβ peptide aggregation by contribution of pyridinium part in the structure of the target system. To reach this purpose, aliphatic carbon chain was employed as cross-linker to endow the target structure with appropriate flexibility and binding affinity towards ChEs. Docking simulation, inhibition mechanism, inhibitory kinetics, anti-Aβ aggregation, nouroprotectivity and toxicity of the selected compounds were investigated to introduce promising multi-targeted-ligands against AD.

2. Results and discussion

2.1. Chemistry

As illustrated in Scheme 1, compound **1a** was prepared via addition of perchloric acid to a solution of 2,4-dihydroxyacetophenone in triethyl orthoformate [43]. The ethyl ester analogue **1b** was prepared from the reaction of 2,4-dihydroxyacetophenone and diethyl oxalate in ethanolic solution of sodium [44]. Also, 2,4-dihydroxyacetophenone underwent cyclization with appropriate benzaldehyde derivatives in the presence of KOH resulting in the formation of chalcone derivatives. The corresponding flavonoid derivatives (**1c-f**) were synthesized by refluxing the chalcone derivative in DMSO with catalytic amount of I_2 for 45 min [45,46]. The intermediates **2a-f** were then synthesized via the reaction of **1a-f** with appropriate amount of dibromoalkanes in acetone solution

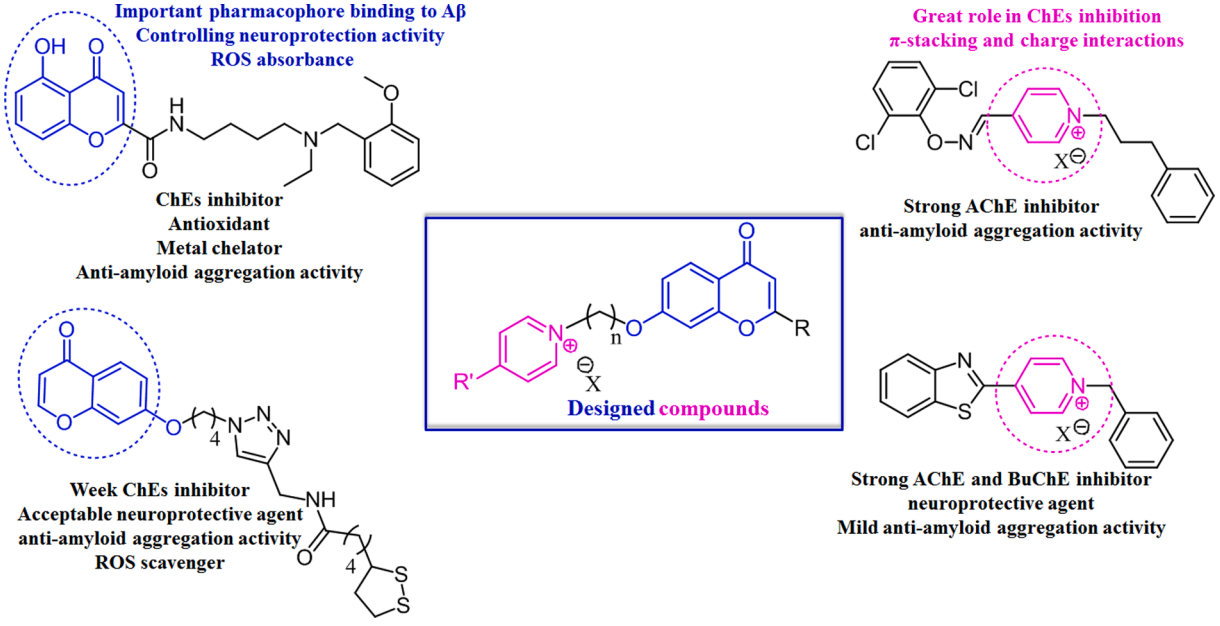

Fig. 1. Design strategy for the preparation of compounds **3**–**26**.

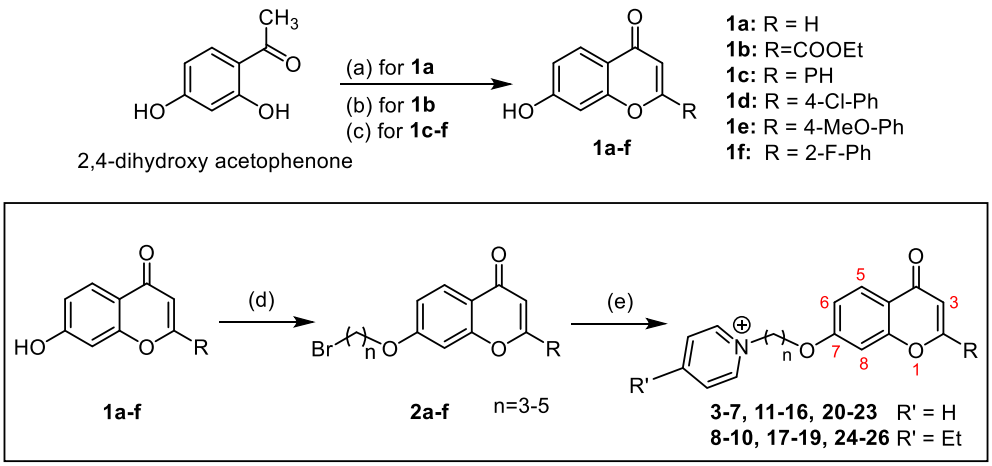

Scheme 1. Synthetic routes to compounds **3**–**26**. Reagents and conditions: (a) $HC(OEt)_3$, 70% $HClO_4$, then H_2O, 100 °C; (b) Na, EtOH (abs), diethyl oxalate, reflux, 1 h; (c) KOH (30%), MeOH, appropriate benzaldehyde derive, stirr, 72 h, then DMSO, I_2, refluxe, 45 min; (d) $Br(CH)_nBr$ (n = 3–5), anhydrous K_2CO_3, acetone, reflux, 4 h; (e) Pyridine, 110 °C, 24 h.

of anhydrous K_2CO_3 under refluxing condition for 4 h. Target compounds **3**–**26** were finally prepared through a reaction between bromoalkoxy intermediates and pyridine derivatives at 110 °C for 24 h.

2.2. Biological assays

2.2.1. Anti-cholinesterase activity

The results of the anticholinesterase activity of the final compounds **3**–**26** are seen in Table 1. The activity was expressed as IC_{50} (μM). For compounds having no appropriate activity, the percent of inhibition was reported at 100 μM. Donepezil as a clinically approved ChEs inhibitor used to treat AD was applied as the standard drug. To investigate the role of linker's length, chromone scaffold was attached to the pyridinium part via 3-, 4- and 5-carbon length (n = 3–5). The role of substituents on the chromone core and pyridinium part was also evaluated. The results clearly confirmed that the presence of substituent at position 2 of the chromone moiety (R) was necessary to improve the inhibitory effect of the compounds. Most of the compounds bearing substituent at position 2 of the chromone ring showed good to moderare AChE inhibitory activity (9.8 μM > IC_{50} > 0.71 μM). The results revealed that 4-carbon chain length (n = 4) could be considered as the optimum length of the linker for AChE inhibition, except for the compounds having no substitution at position 2 of the chromone ring (compounds **3**, **11** and **20**). Shortening or elongation of the linker led to decrease in the activity. Compounds **14**, **16** and **22** were the best AChE inhibitors with IC_{50} value of about 0.7 μM. By comparison of the results, it could be concluded that the presence of substituent (ethyl group) at para position of the pyridinium group improved ChE inhibitory effect of the compounds having 3- or 4-carbon linker length.

Also, most of the compounds had higher BuChE inhibition activity than AChE inhibition activity. 17 out of 23 compounds were more active than donepezil as standard drug and 10 derivatives showed BuChE inhibition activity in nanomolar range (compounds **8**–**10**, **17**–**19** and **21**–**24**). Compound **10** with IC_{50} = 0.006 μM was 566 times more active than standard drug, donepezil (BuChE IC_{50} = 3.4 μM). Such compounds with high selectivity for BuChE may represent an additional advantage for long-term stabilization of cognitive and behavioral symptoms, particularly in progressed or late stage of AD patients, through reducing β-amyloid aggregation and increasing ACh levels in the brain without triggering severe peripheral side effects [8]. Compound **14** as the best AChE inhibitor having appropriate BuChE inhibition activity (IC_{50} = 0.71 and 1.5 μM, respectively) and compound **10** as the best BuChE inhibitor (IC_{50} = 0.006 μM) were selected for further analyses.

Table 1
Inhibitory activity of the synthesized compounds **3**–**26** against AChE and BuChE.

Comp.	n	R'	R	*eel*AChE	Equine serum BuChE	
				IC_{50} (μM)[a]	IC_{50} (μM)	% inhib.[b]
3	3	H	H	24.5 ± 0.6	–	23.6
4	3	H	Ph	3.1 ± 0.1	4.4 ± 0.7	–
5	3	H	4-Cl-Ph	3.1 ± 0.1	1.4 ± 0.2	–
6	3	H	4-OMe-Ph	6.1 ± 0.1	1.3 ± 0.2	–
7	3	H	COOEt	1.0 ± 0.1	82.0 ± 1.7	–
8	3	Et	Ph	2.7 ± 0.1	0.090 ± 0.014	–
9	3	Et	4-Cl-Ph	4.1 ± 0.1	0.097 ± 0.011	–
10	3	Et	4-OMe-Ph	2.5 ± 0.1	0.006 ± 0.001	–
11	4	H	H	32.4 ± 2.5	–	46.3
12	4	H	Ph	2.5 ± 0.2	1.9 ± 0.2	–
13	4	H	2-F-Ph	1.2 ± 0.1	1.1 ± 0.1	–
14	4	H	4-Cl-Ph	0.71 ± 0.1	1.5 ± 0.2	–
15	4	H	4-OMe-Ph	1.4 ± 0.1	1.4 ± 0.2	–
16	4	H	COOEt	0.75 ± 0.1	8.4 ± 1.6	–
17	4	Et	Ph	2.6 ± 0.2	0.012 ± 0.001	–
18	4	Et	4-Cl-Ph	2.5 ± 0.2	0.087 ± 0.005	–
19	4	Et	4-OMe-Ph	9.8 ± 0.6	0.076 ± 0.009	–
20	5	H	H	50.2 ± 1.4	27.8 ± 0.9	–
21	5	H	Ph	6.8 ± 0.5	0.63 ± 0.12	–
22	5	H	4-Cl-Ph	0.79 ± 0.1	0.46 ± 0.06	–
23	5	H	4-OMe-Ph	2.7 ± 0.2	0.99 ± 0.12	–
24	5	Et	Ph	1.1 ± 0.1	0.055 ± 0.001	–
25	5	Et	4-Cl-Ph	24.5 ± 0.8	–	23.6
26	5	Et	4-OMe-Ph	3.1 ± 0.3	4.4 ± 0.8	–
Donepezil	–	–	–	0.023 ± 0.002	3.4 ± 0.2	–

[a] Inhibitor concentration (mean ± SEM of three experiments) for 50% inactivation of AChE (from electrophorus electricus)/BuChE (from equine serum).
[b] Percentage of inhibition of BuChE (mean ± SEM of three experiments).

2.2.2. Kinetic analysis of AChE and BuChE inhibition

The enzyme kinetic study was performed to understand the mode of inhibition. For this purpose, compound **10** and **14** were selected for kinetic analysis of AChE and BuChE inhibition, respectively. The

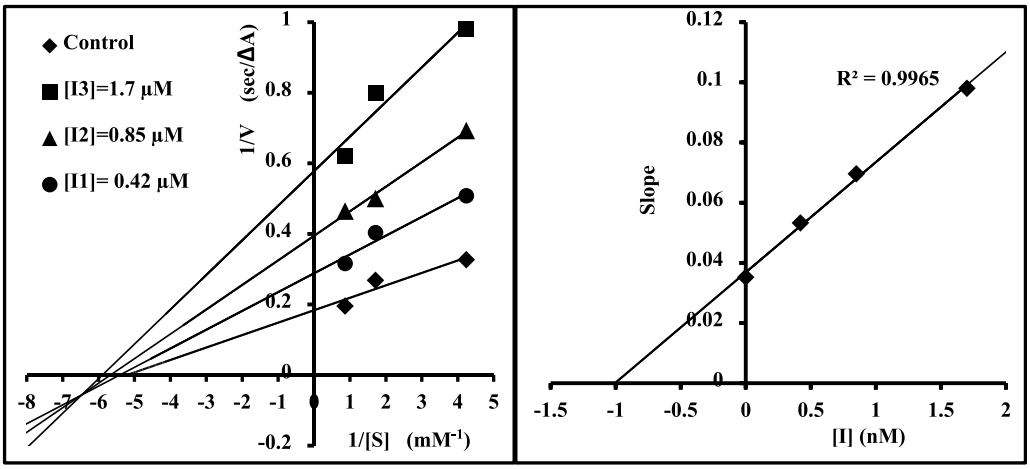

Fig. 2. *Left)* Lineweaver-Burk plot for the inhibition of AChE by compound **14** at different concentrations of substrate (ATCh). *Right)* Secondary plot for calculation of steady-state inhibition constant of compound **14** (K_i = 1.01 µM).

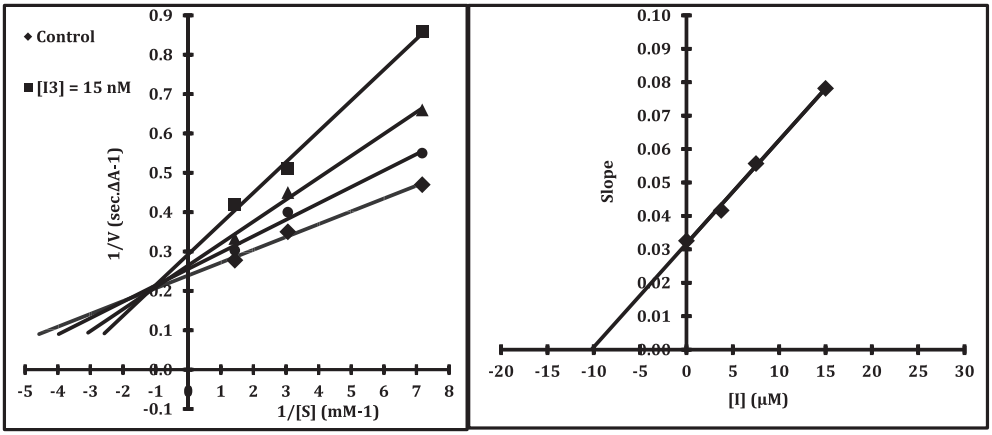

Fig. 3. *Left)* Lineweaver-Burk plot for the inhibition of BuChE by compound **10** at different concentrations of substrate (BuTCh). *Right)* Secondary plot for calculation of steady-state inhibition constant of compound **10** (K_i = 10.25 nM).

Lineweaver-Burke plot for AChE is shown in Fig. 2. Based on the plot, compound **14** showed mixed type of inhibition. The *Ki* value was also calculated using secondary plot (*Ki* = 1.01 µM). Accordingly, the inhibition mode of compound **10** on BuChE was investigated. The results revealed that compound **10** inhibited BuChE in the mixed type manner (Fig. 3). The *Ki* for compound **10** was 10.25 nM. Based on the kinetic results, it could be suggested that both the compounds showed non-competitive inhibition which is kind of reversible inhibition and also could occupy CAS and PAS, simultaneously.

2.2.3. Ligand-protein docking simulation

Docking study was performed to determine the key residues in the ligand involved in the interaction with the enzymes. Compound **14** was used as ligand for AChE and compound **10** for BuChE. The main ligand-enzyme interactions between compound **14** and AChE was illustrated in Fig. 4. As shown, compound **14** occupied both CAS and PAS. The positive charge of pyridine was fascinated to the central anionic site. Trp83 and Glu198 provide negative charge to interact with pyridinium ring. Moreover, Gly116 in the oxyanion hole made an amide-π bond with pyridine. The head of the ligand was directed to the rim of the gorge and engaged in some π-staking. Phenyl ring of chromone stacked against Phe329 in the mid-gorge recognition site. The adjacent ring made two π-staking with Tyr120 and Tyr333 in the PAS of the enzyme. The phenyl at position 2 of the chromone ring was also involved in π-stacking with Tyr333.

Compound **10** was also docked in the active site of BuChE (Fig. 5).

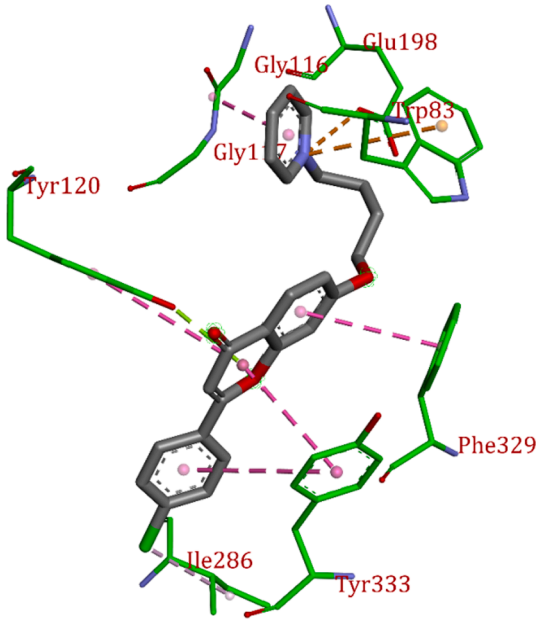

Fig. 4. Interaction of compound **14** with AChE. For simplification the key residues were shown.

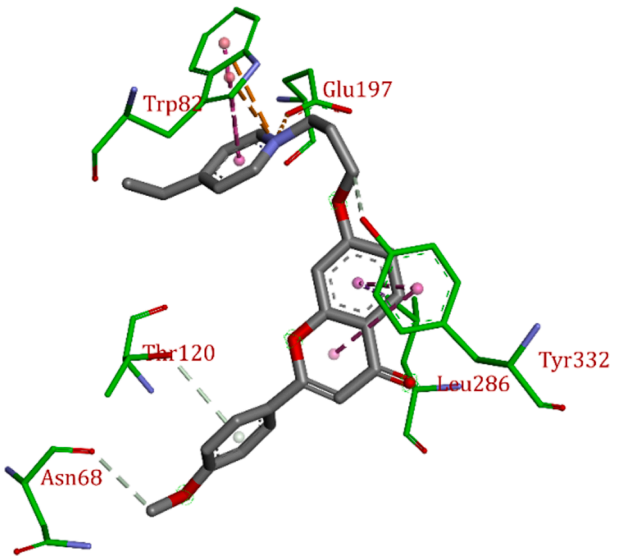

Fig. 5. Interaction of compound **10** with BuChE. For simplification the key residues were shown.

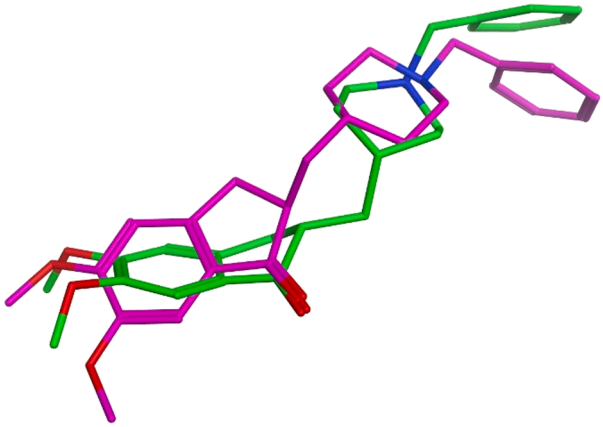

Fig. 6. Redocking of donepezil in the active site of AChE. The green is original ligand (1EVE PDB) and the cyan is the redocked ligand. (For interpretation of the references to color in this figure legend, the reader is referred to the web version of this article.)

Table 2
Inhibition of Aβ self and AChE-induced aggregation by the compound **10** and **14**.

Compound	Inhibition of self-induced Aβ aggregation[a] (%)	Inhibition of AChE-induced Aβ aggregation[b] (%)
10	31.7 ± 1.5	36.6 ± 1.2
14	27.5 ± 1.7	21.8 ± 2.4
Donepezil	15.1 ± 1.8	26.9 ± 3.0

[a] Inhibition of self-induced $A\beta_{1\text{-}42}$ aggregation (25 μM) produced by the tested compound at 10 μM concentration. Values are expressed as means ± SEM of three experiments.

[b] Co-aggregation inhibition of $A\beta_{1\text{-}42}$ and AChE (2 μM, ratio 100:1) by the tested compound at 100 μM concentration was detected by ThT assay. Values are expressed as means ± SEM of three experiments.

Similar to compound **14**, the pyridine ring of compound **10** was adjacent to Trp82 and Glu197 by making attractive charges and the planar chromone ring stacked against Tyr332 in the PAS.

To confirm the robustness of the docking simulations, the original donepezil-AChE complex, retrieved from RCSB (1EVE PDB) was re-docked and its superimposition with the original X-ray structure was rechecked by calculation of the Root Mean Square Deviation (RMSD). The calculated RMSD was 0.42 Å (Fig. 6).

2.2.4. *Inhibitory effects on AChE-induced and self-induced Aβ peptide aggregation*

The potential of compounds **10** and **14** to inhibit Aβ-aggregation was evaluated using thioflavin T (ThT) assay. The obtained results indicated that compounds **10** and **14** displayed significant inhibitory activity against Aβ aggregation (31.7 and 27.5% inhibition, respectively) and compound **10** was about 2-fold more effective than reference drug donepezil (15.1% inhibition, Table 2). The potential of compounds **10** and **14** to inhibit Aβ aggregation induced by AChE were also evaluated (Table 2). Compound **10** showed appropriate inhibition activity toward AChE-induced Aβ aggregation (36.6% inhibition) more than donepezil as standard drug (26.9% inhibition). Compound **14** also exhibited acceptable inhibition activity (21.8% inhibition). The results confirmed appropriate efficacy of the selected compounds to inhibit Aβ aggregation.

2.2.5. *Neuroprotection against H_2O_2-induced cell death in PC12 cells*

The neuroprotective effect of compounds **10** and **14** against neurotoxicity caused by H_2O_2 at the concentrations of 0.1, 1, 5, 10, 20, 50 μM, and prior to treatment with H_2O_2·(150 μM) were evaluated via MTT assay. As seen in Table 3, all the tested concentrations significantly increased PC12 cell viability in a concentration-dependent manner for both compounds. Compound **10** had no significant effect on cell viability just at concentration of 0.1 μM. Notably, the neuroprotective effect of compound **14** at concentrations of 0.1, 1, 5, 10 and 20 μM was higher than that of the reference drug Quercetin.

2.2.6. *Neuroprotective activity against $A\beta_{1\text{-}42}$-induced cytotoxicity in PC12 cells*

It has been reported that Aβ plaques induce oxidative stress on neuronal cells through the formation of free radicals [47]. Therefore, the potential neuroprotective effects of compounds **10** and **14** against $A\beta_{1\text{-}42}$-induced cytotoxicity in PC12 cells were evaluated at the concentrations of 0.01, 0.1, 10 and 100 μM. As seen in Fig. 7, the tested compounds increased cell viability in the presence of Aβ in a concentration-dependent manner. According to the results, compounds **10** and **14** showed significant protective capability with the percentage of cell viability of 79 and 76%, respectively, at the concentrations of 100 μM, higher than reference drug Selegiline (52%) and showed slightly lower protective effect at other concentrations. Compound **10** could protect neuronal cells at concentration of 1–100 μM, greater than compound **14**. The results suggested that target compounds **10** and **14** could efficiently protect neuronal cells against Aβ toxic effects.

2.2.7. *Cytotoxicity effect*

To evaluate the cytotoxic effect of the selected compounds, the MTT based colorimetric assay was employed. The IC_{50} values of compounds **10** and **14** compared with donepezil as the reference drug are seen in Table 4. The results exhibited that both compounds **10** and **14** showed lower cytotoxic effect on normal cell (HDF) compared with two cancer cell lines (Table 4). In addition, compound **10** was somehow more toxic than compound **14** against all applied three cell lines. Interestingly, the cytotoxic effect of the selected compounds was lower than donepezil as a clinically approved standard drug.

2.2.8. *ADMET prediction*

The ADMET (absorption, distribution, metabolism, excretion and toxicity) property of the compounds was predicted using the SwissADME web server (http://www.swissadme.ch) [48]. Based on the predicted values, all compounds could be able to penetrate brain and therefore could be considered as CNS-active compounds, except for compound **25**. Also, the compounds showed well gastrointestinal (GI) absorption property (Table 5). The computed physicochemical descriptors, pharmacokinetic properties and druglike nature of compounds

Table 3
The protective effect of compound **10** and **14** against H_2O_2-induced injury in PC12 cell line at different concentrations.

Compound	n	R	R'	PC12 cells viability (% of control)						
				H_2O_2	0.1 μM	1 μM	5 μM	10 μM	20 μM	50 μM
10	3	Et	4-OMe-Ph	33.0 ± 1.0	34.4 ± 0.8 ^{ns}	37.7 ± 1.5***	42.3 ± 0.9***	53.4 ± 1.3***	58.2 ± 0.4***	47.2 ± 1.8***
14	4	H	4-Cl-Ph	33.2 ± 1.3	47.7 ± 1.8***	57.8 ± 1.3***	61.9 ± 1.1***	66.1 ± 1.3***	69.9 ± 6.5***	49.7 ± 1.3***
Quercetin	–	–	–	31.9 ± 1.7	37.1 ± 2.0***	43.6 ± 1.6***	46.6 ± 0.4***	51.3 ± 1.6***	56.2 ± 2.0***	59.9 ± 2.3***

Cell viability was determined using MTT assay protocol. Data are expressed as the mean ± SEM of three independent replicates. The significant ($^{***}p < 0.001$) and not significant (ns) values with respect to the H_2O_2 group.

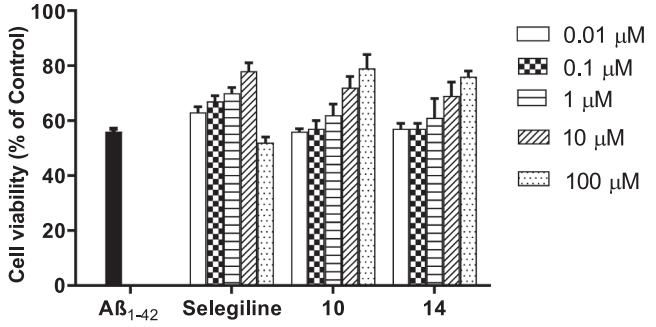

Fig. 7. Protective effects of compounds **10** and **14** on cell injury induced by $A\beta_{1\text{-}42}$ in PC12 cells. All groups were treated with 25 μM $A\beta_{1\text{-}42}$ except for the control group. The synthetic compounds and Selegiline were pre-incubated at various concentrations (0.01–100 μM) in serum-free media for 24 h before the addition of Aβ peptide. Cell viability is expressed as the mean percentage of viable cells compared with the untreated cells. The data are the mean ± SE. (See supporting information for details, Table S1).

Table 4
Calculated IC_{50} (μM) for compounds **10** and **14** and donepezil against PC12 (rat pheochromocytoma), HepG2 (human hepatocarcinoma) and human dermal fibroblast (HDF).

Compound	PC12	HepG2	HDF
10	336.2 ± 9.4	281.1 ± 7.2	543.2 ± 19.7
14	376.4 ± 10.1	312.9 ± 12.0	628.4 ± 19.6
Donepezil	314.2 ± 8.7	256.2 ± 4.9	363.4 ± 8.7

IC_{50}s were determined using MTT assay protocol. Data are expressed as the mean ± SEM of three independent replicates.

10 and **14** as the most promising compound have been also provided in supporting information (see supporting information, Figs. S1–S4).

3. Conclusion

In this work a series of chromone derivatives bearing pyridinium part cross-linked to each other via flexible aliphatic carbon chain was prepared and evaluated as multi-target directed ligands against AD. Most of the compounds showed good to moderate AChE inhibitory activity and excellent BuChE inhibition effect. A series of the compounds (17 derivatives, compounds **5**, **6**, **8-10**, **12-15**, **17-19**, **21-24**) exhibited strong BuChE inhibitory effect, more than standard drug, donepezil. Especially, compound **10** was 566 times more active than donepezil. The most active ChE inhibitors (compounds **10** and **14**) revealed high neuroprotective activity against H_2O_2-induced cytotoxicity in PC12 cells. Especially, compound **14** as the best AChE inhibitor (IC_{50} = 0.71 μM) showed higher neuroprotective activity than reference drug, Quercetin. Both compounds could efficiently protect neuronal cells against Aβ toxic effects and were more active than the standard drug, Selegiline, to protect PC12 cells against $A\beta_{1\text{-}42}$-induced cytotoxicity. Interestingly, the selected compounds revealed valuable self- and AChE-induced anti-Aβ aggregation activity, especially compound **10** was more active than donepezil as standard drug. All the aforementioned findings suggest that these new hybrids of chromone and pyridinium parts could be considered as promising multifunctional agents for further studies in the field of AD. Study on the other potency of the target compounds in animal models will be the objective of our future works.

4. Experimental

4.1. Chemistry

All starting materials and solvents for the synthesis were purchased commercially from various suppliers and used without any purification. The solvents were dehydrated according to the standard methods. The melting points were recorded on a Kofler hot stage apparatus. The purity of all products was confirmed by TLC, FTIR, ^{1}H NMR and ^{13}C NMR. TLC was conducted on silica gel 250 μm, F254 plates (Merck). FTIR spectra were recorded on a Bruker tensor 27 FT/IR spectrophotometer (KBr disks), ^{1}H NMR and ^{13}C NMR spectra were recorded on a Brucker 500 MHz NMR and Bruker avence 250 MHz spectrometer using dimethylsulfoxide (DMSO-d_6) as solvent. The chemical shifts (δ) and coupling constants (J) were presented in parts per million (ppm) and Hertz (Hz). The elemental analysis of the compounds (C, H, and N) was determined with CHN-Rapid Heraeus Elemental Analyzer agreed to within ±0.4% of the calculated value. HPLC (Youngling 9100, South Korea) was served to plot the chromatogram using a C18 column (150 × 4.6 mm) and the mobile phase consisted of acetonitrile:water (60:40) was employed. Methanol was applied as solvent. The flow rate was 1.2 mL/min. Ultraviolet absorption was read at 262 nm and the compound was identified using a diode array detector.

4.1.1. General procedure for the preparation of compound *1a*

To a stirring solution of 2,4-dihydroxyacetophenone (1 mmol) in triethyl orthoformate (1 mL), 70% perchloric acid (0.1 mL) was added dropwise. The dark mixture was stirred until it was cooled to room temperature. The anhydrous diethyl ether (3 mL) was added and then a brown precipitate was filtered. The solid dissolved in hot water (2 mL), and refluxed for 5 min. The mixture was allowed to cool overnight. A dark product was filtered and recrystallized with water/ethanol [43].

4.1.2. General procedure for the preparation of compound *1b*

A mixture of 2,4-dihydroxyacetophenone (2.28 g) and diethyl oxalate (7.3 g) in ethanol (10 mL) was added to a solution of in situe prepared sodium ethoxide by adding 1.8 g sodium to EtOH (100 mL) and the solution was then refluxed for 1 h. The solution was acidified and the white precipitate was filtered off, then the solution was extracted with ethylacetate and water. The product was recrystallized from ethylacetate [44].

4.1.3. General procedure for the preparation of compounds *1c-f*

2,4-dihydroxyacetophenone (10 mmol) was mixed with appropriate benzaldehyde derivatives (10 mmol) in the presence of KOH solution (30%, in 30 mL methanol) and stirred for 72 h. After completion of the reaction (TLC control), the mixture was acidified and the product extracted with ethylacetate/water and purified by column chromatography [45]. Then, the purified chalcone was refluxed in DMSO with catalytic amount of I_2 for 45 min. The mixture was washed with water and the product was extracted with ethylacetate. The solvent was

Table 5
The ADMET properties of the compounds predicted using SwissADME web-based server.

Compound	n	R'	R	TPSA (Å^2)	Consensus logP	BBB permeation	GI absorption
3	3	H	H	43.32	1.79	+	+
4	3	H	Ph	43.32	3.26	+	+
5	3	H	4-Cl-Ph	43.32	3.81	+	+
6	3	H	4-OMe-Ph	52.55	3.27	+	+
7	3	H	COOEt	69.62	2.10	+	+
8	3	Et	Ph	43.32	3.93	+	+
9	3	Et	4-Cl-Ph	43.32	4.43	+	+
10	3	Et	4-OMe-Ph	52.55	3.94	+	+
11	4	H	H	43.32	2.14	+	+
12	4	H	Ph	43.32	3.59	+	+
13	4	H	2-F-Ph	43.32	3.75	+	+
14	4	H	4-Cl-Ph	43.32	4.15	+	+
15	4	H	4-OMe-Ph	52.55	3.58	+	+
16	4	H	COOEt	69.62	2.41	+	+
17	4	Et	Ph	43.32	4.25	+	+
18	4	Et	4-Cl-Ph	43.32	4.76	+	+
19	4	Et	4-OMe-Ph	52.55	4.21	+	+
20	5	H	H	43.32	2.56	+	+
21	5	H	Ph	43.32	3.92	+	+
22	5	H	4-Cl-Ph	43.32	4.37	+	+
23	5	H	4-OMe-Ph	52.55	3.93	+	+
24	5	Et	Ph	43.32	4.57	+	+
25	5	Et	4-Cl-Ph	43.32	5.91	–	+
26	5	Et	4-OMe-Ph	52.55	4.56	+	+
Donepezil	–	–	–	33.77	4.00	+	+

removed under vacuum [46].

4.1.4. General procedure for the preparation of bromoalkoxy intermediates *2a-f*

The hydroxylayed chromone derivative (1 mmol) with appropriate dibromoalkane (10 mmol) and anhydrous K_2CO_3 (2 mmol) was refluxed in acetone (5 mL) for 4 h. After cooling, the reaction mixture was filtered and the organic phase was evaporated under reduced pressure. The obtained residue was triturated with *n*-hexane to give the product as white solid [49].

4.1.5. General procedure for the preparation of the final compounds *(3–26)*

The bromoalkoxy intermediate (**2a-f**, 1 mmol) was stirred in pyridine (15 mL) at 110 °C for 24 h. After completion of the reaction (TLC control), the reaction mixture was put in ice bath and cold ether was added to the mixture. Then, the precipitated product was filtered off and washed with ether [50].

*4.1.5.1. 1-(3-((4-Oxo-4H-chromen-7-yl) oxy) propyl) pyridin-1-ium **(3)**.* Pink solid; yield 90%; mp 164–166 °C; IR (KBr, cm^{-1}) υ_{max}: 3039–3093 (C—H aromatic), 2882–2941 (C—H), 1636 (C═O), 1045 (C—O); ^{1}H NMR (DMSO-d_6, 500 MHz) δ 2.45 (bs, 2H, CH_2), 4.25 (t, 2H, J = 5.6 Hz, O—CH_2), 4.83 (t, 2H, J = 7.0 Hz, N—CH_2), 6.28 (d, 1H, J = 6.0 Hz, H_3), 6.84 (d, 1H, J = 7.5 Hz, H_6), 7.07 (s, 1H, H_8), 7.91 (d, 1H, J = 9.0 Hz, H_5), 8.17 (t, 2H, J = 7.0 Hz, pyridine), 8.24 (d, 1H, J = 5.5 Hz, H_2), 8.63 (t, 1H, J = 8.0 Hz, pyridine), 9.16 (d, 2H, J = 6.0 Hz, pyridine); ^{13}C NMR (DMSO-d_6, 125 MHz) δ 26.4, 28.6, 31.9, 50.0, 109.4, 114.4, 122.3, 126.2, 127.8, 128.0, 128.7, 144.2, 162.9, 196.0; Anal. Calcd for $C_{17}H_{16}NO_3$ (282.32): C, 72.33; H, 5.71; N, 4.96. Found: C, 72.55; H, 5.94; N, 5.18.

*4.1.5.2. 1-(3-((4-Oxo-2-phenyl-4H-chromen-7-yl) oxy) propyl) pyridin-1-ium **(4)**.* Yellow solid; yield 90%; mp 95–96 °C; IR (KBr, cm^{-1}) υ_{max}: 3051 (C—H aromatic), 2925 (C—H), 1604 (C═O), 1172 (C—O); 1H NMR (DMSO-d_6, 500 MHz) δ 2.5 (bs, 2H, CH_2), 4.28 (t, 2H, J = 5.0 Hz, O—CH_2), 4.86 (t, 2H, J = 6.0 Hz, N—CH_2), 6.84 (d, 1H, J = 9.0 Hz, H_6), 6.97 (s, 1H, H_3), 7.27 (s, 1H, H_8), 7.37 (t, 2H, J = 6.0 Hz, $H_{1',5'}$), 7.58 (m, 3H, $H_{2',3',4'}$), 8.08 (d, 1H, J = 7.0 Hz, H_5), 8.18 (t, 2H, J = 6.8 Hz, pyridine), 8.64 (t, 1H, J = 7.5 Hz, pyridine), 9.20 (d, 2H, J = 6.0 Hz, pyridine); ^{13}C NMR (DMSO-d_6, 125 MHz) δ 29.75, 58.76, 65.9, 101.5, 106.8, 114,9, 117.3, 126.2, 128.0, 129.1, 131.1, 131.8, 145.1, 145.7, 157.4, 162.2, 162.5, 176.4. Anal. Calcd for $C_{23}H_{20}NO_3$ (358.41): C, 77.08; H, 5.62; N, 3.91. Found: C, 77.92; H, 5.82; N, 3.84.

*4.1.5.3. 1-(3-((2-(4-Chlorophenyl)-4-oxo-4H-chromen-7-yl) oxy) propyl) pyridin-1-ium **(5)**.* Yellow solid; yield 90%; mp 150–151 °C; IR (KBr, cm^{-1}) υ_{max}: 2852–2926 (C—H), 1628 (C═O), 1007 (C—O); ^{1}H NMR (DMSO-d_6, 250 MHz) δ 2.47 (bs, 2H, CH_2), 4.25 (bs, 2H, O—CH_2), 4.85 (t, 2H, J = 7.5 Hz, N—CH_2), 6.79 (d, 1H, J = 8.7 Hz, H_6), 6.94 (s, 1H, H_3), 7.23 (s, 1H, H_8), 7.59 (d, 2H, J = 8.2 Hz, $H_{1',5'}$), 7.85 (d, 1H, J = 8.7 Hz, H_5), 8.05 (d, 2H, J = 8.5 Hz, pyridine), 8.16 (t, 2H, J = 6.5 Hz, $H_{2',4'}$), 8.62 (t, 1H, J = 7.5 Hz, pyridine), 9.20 (d, 2H, J = 5.0 Hz, pyridine); ^{13}C NMR (DMSO-d_6, 62.9 MHz) δ 30.1, 59.0, 66.3, 101.9, 107.5, 115.1, 117.6, 126.64, 128.45, 129.2, 129.61, 130.4, 131.5, 136.9, 145.5, 146.1, 157.7, 161.4, 162.9, 176.7. Anal. Calcd for $C_{23}H_{19}ClNO_3$ (392.85): C, 70.32; H, 4.87; N, 3.57. Found: C, 70.12; H, 5.13; N, 3.31.

*4.1.5.4. 1-(3-((2-(4-Methoxyphenyl)-4-oxo-4H-chromen-7-yl) oxy) propyl) pyridin-1-ium **(6)**.* Yellow solid; yield 95%; mp 130–132 °C; IR (KBr, cm^{-1}) υ_{max}: 3057 (C—H aromatic), 2927 (C—H), 1621 (C═O), 1023 (C—O); 1H NMR (DMSO-d_6, 250 MHz,) δ 2.47 (bs, 2H, CH_2), 3.82 (s, 3H, OCH_3), 4.25 (t, 2H, J = 5.0 Hz, O—CH_2), 4.84 (t, 2H, J = 6.5 Hz, N—CH_2), 6.76–6.89 (m, 2H, $H_{3,6}$), 7.07 (d, 2H, J = 8.7 Hz, $H_{2',4'}$), 7.20 (d, 1H, J = 2.0 Hz, H_8), 7.84 (d, 1H, J = 2.5 Hz, H_5), 7.99 (d, 2H, J = 8.7 Hz, $H_{1',5'}$), 8.15 (t, 2H, J = 6.7 Hz, pyridine), 8.61 (t, 1H, J = 7.7 Hz, pyridine), 9.18 (d, 2H, J = 7.2 Hz, pyridine); ^{13}C NMR (DMSO-d_6, 62.9 MHz) δ 30.1, 55.9, 59.1, 66.2, 101.8, 105.6, 114.98, 117.6, 123.6, 126.5, 128.4, 145.5, 146.1, 157,6, 162.4, 162.7, 176.7. Anal. Calcd for $C_{24}H_{22}NO_4$ (388.44): C, 74.21; H, 5.71; N, 3.61. Found: C, 74.51; H, 5.82; N, 3.82.

*4.1.5.5. 1-(3-((2-(Ethoxycarbonyl)-4-oxo-4H-chromen-7-yl) oxy) propyl) pyridin-1-ium **(7)**.* Yellow solid; yield 80%; mp 89–90 °C; IR (KBr, cm^{-1}) υ_{max}: 3053 (C—H aromatic), 2936–2968 (C—H), 1732 (C═O), 1017 (C—O); 1H NMR (DMSO-d_6, 500 MHz) δ 1.33 (t, 3H, J = 6 Hz, O—CH_2—$C\underline{H}_3$), 2.48 (bs, 2H, CH_2), 4.28 (bs, 2H, O—CH_2), 4.37 (bs, 2H, O—$C\underline{H}_2$—CH_3), 4.84 (bs, 2H, N—CH_2), 6.88 (m, 2H, $H_{6,8}$), 7.19 (m, 1H, H_3), 7.91 (d, 1H, J = 9.0 Hz, H_5) , 8.17 (m, 2H, pyridine), 8.63 (t, 1H, J = 7.5 Hz, pyridine), 9.18 (d, 2H, J = 5.0 Hz, pyridine); ^{13}C NMR

(DMSO-d_6, 125 MHz) δ 13.9, 29.6, 58.6, 62.7, 66.0, 101.5, 114.0, 115.9, 117.8, 126.4, 128.0, 145.1, 145.7, 152.0, 157.2, 160.0, 163.2, 176.3. Anal. Calcd for $C_{20}H_{20}NO_5$ (354.38): C, 67.79; H, 5.69; N, 3.95. Found: C, 67.41; H, 5.83; N, 3.76.

4.1.5.6. 4-Ethyl-1-(3-((4-oxo-2-phenyl-4H-chromen-7-yl) oxy) propyl) pyridin-1-ium ***(8)***. Yield 60%; Brown solid; mp 134–135 °C; IR (KBr, cm^{-1}) υ_{max}: 3050 (C—H aromatics), 2924 (C—H), 1629 (C═O), 1173 (C—O). ^{1}H NMR (DMSO-d_6, 250 MHz) δ 1.22 (t, 3H, J = 7.5 Hz, CH_3), 2.60 (m, 2H, CH_2), 2.89 (bs, 2H, CH_3—C<u>H</u>$_2$), 4.28 (bs, 2H, O—CH_2), 4.75 (bs, 2H, N—CH_2), 6.98 (s, 1H, H_3), 7.05 (bs, 1H, H_6), 7.20 (s, 1H, H_8), 7.57 (m, 3H, $H_{2', 3', 4'}$), 7.77–8.18 (m, 4H, pyridine and H_5), 9.01 (d, 2H, J = 6.0 Hz, pyridine); ^{13}C NMR (DMSO-d_6, 62.9 MHz) δ 13.9, 28.4, 29.9, 58.3, 66.3, 101.9, 107.2, 115.1, 126.6, 126.8, 127.5, 129.5, 132.2, 144.7, 164.3, 176.8. Anal. Calcd for: $C_{25}H_{24}NO_3$ (386.46): C, 77.70; H, 6.26; N, 3.62. Found: C, 77.92; H, 6.03; N, 3.45.

4.1.5.7. 1-(3-((2-(4-Chlorophenyl)-4-oxo-4H-chromen-7-yl)oxy)propyl)-4-ethylpyridin-1-ium ***(9)***. Yield 60%; off Brown solid; mp 144–145 °C; IR (KBr, cm^{-1}) υ_{max}: 3023 (C—H aromatics), 2968 (C—H), 1633 (C═O), 1174 (C—O). ^{1}H NMR (DMSO-d_6, 250 MHz) δ 1.25 (t, 3H, CH_3), 2.60 (2H, CH_2), 2.91 (2H, CH_3—C<u>H</u>$_2$), 4.25 (bs, 2H, O—CH_2), 4.75 (bs, 2H, N—CH_2), 6.80 (d, 1H, J = 8.2 Hz, H_6), 6.98 (s,1H, H_3), 7.22 (bs, 1H, H_8), 7.62 (d, 2H, J = 8.5 Hz, $H_{1', 5'}$), 7.87 (d, 2H, J = 9.0 Hz, $H_{2', 4'}$), 8.04 (m, 2H, pyridine), 8.42 (d, 1H, J = 5.5 Hz, H_5), 9.05 (d, 2H, J = 6.2 Hz, pyridine); ^{13}C NMR (DMSO-d_6, 62.9 MHz) δ 13.9, 28.4, 30.0, 58.3, 66.3, 101.9, 107.5, 115.2, 117.6, 123.1, 126.6, 127.5, 128.4, 129.6, 130.4, 136.9, 144.7, 149.1, 157.7, 161.4, 162.9, 164.3, 176.7. Anal. Calcd for: $C_{25}H_{23}ClNO_3$ (420.91): C, 71.34; H, 5.51; N, 3.33. Found: C, 71.12; H, 5.88; N, 3.61.

4.1.5.8. 4-Ethyl-1-(3-((2-(4-methoxyphenyl)-4-oxo-4H-chromen-7-yl) oxy)propyl)pyridin-1-ium ***(10)***. Yield 70%; off yellow solid; mp 100–102 °C; IR (KBr, cm^{-1}) υ_{max}: 3046 (C—H aromatic), 2972 (C—H), 1640 (C═O), 1179 (C—O). ^{1}H NMR (DMSO-d_6, 250 MHz) δ 1.23 (t, 3H, J = 5.5 Hz, CH_3), 1.96 (bs, 2H, CH_2), 2.91 (bs, 2H, CH_3—C<u>H</u>$_2$), 3.84 (s, 3H, OCH_3), 4.25 (bs, 2H, O—CH_2), 4.76 (bs, 2H, N—CH_2), 6.81–6.85 (m, 2H, $H_{3,6}$), 7.18–727 (m, 3H, H_8 and $H_{2',4'}$), 7.86–8.03 (m, 5H, H_5, $H_{1',5'}$ and pyridine), 9.02 (d, 2H, J = 6.0 Hz, pyridine); ^{13}C NMR (DMSO-d_6, 62.9 MHz) δ 13.9, 28.4, 29.9, 56.0, 58.3, 66.3, 101.9, 105.7, 115.0, 127.5, 128.4, 144.7, 149.0, 162.7, 164.3, 176.7. Anal. Calcd for: $C_{26}H_{26}NO_4$ (416.49): C, 74.98; H, 6.29; N, 3.36. Found: C, 75.06; H, 6.56; N, 3.62.

4.1.5.9. 1-(4-((4-Oxo-4H-chromen-7-yl) oxy) butyl) pyridin-1-ium ***(11)***. Yellow solid; yield 92%; mp 140–143 °C; IR (KBr, cm^{-1}) υ_{max}: 3056 (C—H aromatic), 2925 (C—H), 1625 (C═O), 1074 (C—O); 1H NMR (DMSO-d_6, 500 MHz,) δ 1.78 (t, 2H, J = 8.5 Hz, CH_2), 2.10 (t, 2H, J = 6.5 Hz, CH_2), 4.16 (t, 2H, J = 6.0 Hz, O—CH_2), 4.69 (t, 2H, J = 7.5 Hz, N—CH_2), 6.27 (d, 1H, J = 6.0 Hz, H_3), 7.04 (d, 1H, J = 9.0 Hz, H_6), 7.13 (s, 1H, H_8), 7.93 (d, 1H, J = 9.0 Hz, H_5), 8.16 (t, 2H, pyridine), 8.22 (d, 1H, J = 6.0 Hz, H_2), 8.61 (t, 1H, J = 6.0 Hz, pyridine), 9.12 (d, 2H, J = 6.0 Hz, pyridine); ^{13}C NMR (DMSO-d_6, 125 MHz) δ 24.9, 27.6, 60.3, 67.8, 101.3, 112.1, 115.0, 118.0, 126.4, 128.1, 144.8, 145.5, 156.6, 157.7, 162.9, 175.7. Anal. Calcd for $C_{18}H_{18}NO_3$ (296.34): C, 72.95; H, 6.12; N, 4.73. Found: C, 72.86; H, 6.31; N, 4.62.

4.1.5.10. 1-(4-((4-Oxo-2-phenyl-4H-chromen-7-yl) oxy) butyl) pyridin-1-ium ***(12)***. Yellow solid; yield 92%; mp 102–104 °C; IR (KBr, cm^{-1}) υ_{max}: 3050 (C—H aromatic), 2942 (C—H), 1628 (C═O), 1013 (C—O); ^{1}H NMR (DMSO-d_6, 500 MHz) δ 1.81 (bs, 2H, CH_2), 2.12 (bs, 2H, CH_2), 4.19 (t, 2H, J = 9.4 Hz, O—CH_2), 4.73 (t, 2H, J = 8.5 Hz, N—CH_2), 6.97 (s, 1H, H_3), 7.05 (d, 1H, J = 8.5 Hz, H_6), 7.33 (s, 1H, H_8), 7.58 (m, 3H, $H_{2', 3', 4'}$), 7.93 (d, 1H, J = 8.5 Hz, H_5), 8.08 (d, 2H, J = 9.5 Hz, $H_{1', 5'}$), 8.62 (t, 2H, J = 7.5 Hz, pyridine), 9.14–9.17 (m, 3H, pyridine); ^{13}C NMR (DMSO-d_6, 125 MHz) δ 25.0, 27.6, 60.3, 67.8, 101.5, 106.8, 115.0, 117.1, 126.2, 128.2, 129.1, 131.7, 144.8, 145.6, 157.5, 162.2, 163.0, 176.4. Anal. Calcd for $C_{24}H_{22}NO_3$ (372.44): C, 77.40; H, 5.95; N, 3.76. Found: C, 77.65; H, 5.76; N, 3.91.

4.1.5.11. 1-(4-((2-(2-Fluorophenyl)-4-oxo-4H-chromen-7-yl) oxy) butyl) pyridin-1-ium ***(13)***. Brown solid; yield 96%; mp 92–93 °C; IR (KBr, cm^{-1}) υ_{max}: 3058 (C—H aromatic), 2852–2924 (C—H), 1743 (C═O), 1029 (C—O); ^{1}H NMR (DMSO-d_6, 500 MHz,) δ 1.80 (bs, 2H, CH_2), 2.12 (bs, 2H, CH_2), 4.18 (bs, 2H, O—CH_2), 4.71 (t, 2H, J = 5.5 Hz, N—CH_2), 6.71 (s,1H, H_3), 7.07 (d, 1H, J = 8 Hz, H_6), 7.27 (s, 1H, H_8), 7.48–7.43 (m, 2H, $H_{2', 4'}$), 7.66–7.67 (m, 1H, H_5), 7.95 (d, 1H, J = 8.5 Hz, $H_{1'}$) , 8.00 (t, 1H, J = 7.5 Hz, $H_{3'}$), 8.18 (t, 2H, J = 6.5 Hz, pyridine), 8.62 (t, 1H, J = 7.5 Hz, pyridine), 9.15 (d, 2H, J = 5.0 Hz, pyridine); ^{13}C NMR (DMSO-d_6, 125 MHz) δ 25.0, 27.6, 60.4, 67.8, 101.4, 115.3, 116.9, 117.0, 125.2, 126.3, 128.2, 129.5, 144.8, 156.1 (C-F), 157.6, 163.2, 176.1. Anal. Calcd for $C_{24}H_{21}FNO_3$ (390.43): C, 73.83; H, 5.42; N, 3.59. Found: C, 73.43; H, 5.22; N, 3.44.

4.1.5.12. 1-(4-((2-(4-Chlorophenyl)-4-oxo-4H-chromen-7-yl) oxy) butyl) pyridin-1-ium ***(14)***. Yellow solid; yield 88%; HPLC tR 3.437 min (99%); mp 111–112 °C; IR (KBr, cm^{-1}) υ_{max}: 3038 (C—H aromatic), 2957 (C—H), 1642 (C═O), 1013 (C—O); ^{1}H NMR (DMSO-d_6, 500 MHz) δ 1.8 (m, 2H, CH_2), 2.13 (bs, 2H, CH_2), 4.19 (t, 2H, J = 6.0 Hz, O—CH_2), 4.74 (t, 2H, J = 7.5 Hz, N—CH_2), 6.99 (s,1H, H_3), 7.04 (d,1H, J = 9.0 Hz, H_6), 7.32 (s,1H, H_8), 7.63 (d, 2H, J = 8.0 Hz, $H_{1', 5'}$), 7.76 (d, 2H, J = 8 Hz, $H_{2', 4'}$), 7.92 (d, 1H, J = 9.5 Hz, H_5), 8.19 (t, 2H, J = 6.0 Hz, pyridine), 8.63 (t, 1H, J = 8.0 Hz, pyridine), 9.18 (d, 2H, J = 6 Hz, pyridine); ^{13}C NMR (DMSO-d_6, 125 MHz) δ 25.0, 27.6, 60.4, 67.8, 101.5, 107.1, 115.1, 117.1, 123.9, 126.2, 128.0, 128.2, 136.2, 144.8, 149.6, 157.4, 161.0, 163.1, 174.4. Anal. Calcd for $C_{24}H_{21}ClNO_3$ (406.89): C, 70.85; H, 5.20; N, 3.44. Found: C, 70.93; H, 5.21; N, 3.13.

4.1.5.13. 1-(4-((2-(4-Methoxyphenyl)-4-oxo-4H-chromen-7-yl) oxy) butyl) pyridin-1-ium ***(15)***. Yellow solid; yield 90%; mp 190–191 °C; IR (KBr, cm^{-1}) υ_{max}: 3045 (C—H aromatic), 2852–2926 (C—H), 1630 (C═O), 1025 (C—O); ^{1}H NMR (DMSO-d_6, 500 MHz,) δ 1.81 (t, 2H, J = 8.0 Hz, CH_2), 2.12 (t, 2H, J = 6.0 Hz, CH_2), 3.85 (s, 3H, OCH_3), 4.19 (t, 2H, J = 5.0 Hz, O—CH_2), 4.74 (t, 2H, J = 7.5 Hz, N—CH_2), 6.86 (s, 1H, H_3), 7.02 (d, 1H, J = 13.6 Hz, H_6), 7.11 (d, 2H, J = 8.5 Hz, $H_{2', 4'}$), 7.30 (s, 1H, H_8), 7.91 (d, 1H, J = 8.5 Hz, H_8), 8.04 (d, 2H, J = 10.0 Hz, $H_{1', 5'}$), 8.19 (t, 2H, J = 7.0 Hz, pyridine), 8.63 (t, 1H, J = 7.5 Hz, pyridine), 9.18 (d, 2H, J = 6.0 Hz, pyridine); ^{13}C NMR (DMSO-d_6, 125 MHz) δ 25.0, 27.6, 55.5, 55.6, 60.3, 67.80, 101.4, 105.3, 114.8, 114.8, 117.1, 123.3, 126.1, 128.0, 128.2, 144.8, 145.6, 157.3, 162.0, 162.2, 162.9, 176.3. Anal. Calcd for $C_{25}H_{24}NO_4$ (402.47): C, 71.61; H, 6.01; N, 3.48. Found: C, 71.82; H, 5.90; N, 3.78.

4.1.5.14. 1-(4-((2-(Ethoxycarbonyl)-4-oxo-4H-chromen-7-yl) oxy) butyl) pyridin-1-ium ***(16)***. Yellow solid; yield 85%; mp 95–96 °C; IR (KBr, cm^{-1}) υ_{max}: 3053 (C—H aromatic), 2936 (C—H), 1732 (C═O), 1083 (C—O); ^{1}H NMR (DMSO-d_6, 250 MHz,) δ 1.30 (t, 3H, J = 7.5 Hz, CH_3), 1.76 (bs, 2H, CH_2), 1.96 (bs, 2H, CH_2), 4.16 (bs, 2H, CH_3—C<u>H</u>$_2$), 4.36 (t, 2H, J = 5.0 Hz, O—CH_2), 4.72 (bs, 2H, N—CH_2), 6.83 (s, 1H, H_3), 7.04 (d, 1H, J = 8.7 Hz, H_6), 7.17 (s, 1H, H_8), 7.88(d, 1H, J = 9.2 Hz, H_5), 8.18 (bs, 2H, pyridine), 8.60 (t, 1H, J = 5.7 Hz, pyridine), 9.18 (d, 2H, J = 5.2 Hz, pyridine); ^{13}C NMR (DMSO-d_6, 62.9 MHz) δ 14.3, 25.3, 28.0, 60.7, 63.1, 68.4, 101.8, 114.4, 116.5, 118.0, 126.8, 128.5, 145.2, 150.0, 150.3, 157.7, 164.2, 176.7. Anal. Calcd for $C_{21}H_{22}NO_5$ (368.41): C, 68.47; H, 6.02; N, 3.80. Found: C, 68.31; H, 5.37; N, 4.10.

4.1.5.15. 4-Ethyl-1-(4-((4-oxo-2-phenyl-4H-chromen-7-yl) oxy) butyl) pyridin-1-ium ***(17)***. Yield 83%; off Brown solid; mp 136–137 °C; IR (KBr, cm^{-1}) υ_{max}: 3037 (C—H aromatic), 2936 (C—H), 1712 (C═O), 1176 (C—O). ^{1}H NMR (DMSO-d_6, 250 MHz) δ 1.22 (t, 3H, J = 7.5 Hz, CH_3),

1.70 (bs, 2H, CH_2), 2.10 (bs, 2H, CH_2), 2.86 (q, 2H, J = 7.5 Hz, CH_3—C$\underline{H}_2$), 4.20 (bs, 2H, O—CH_2), 4.66 (d, 2H, J = 7.5 Hz, N—CH_2), 6.91 (s, 1H, H_3), 7.01 (bs, 1H, H_6), 7.22–7.56 (m, 4H, H_8 and $H_{2'\text{-}4'}$), 8.07–8.02 (m, 5H, $H_{1',5'}$, H_5 and pyridine), 9.05 (t, 2H, J = 6.2 Hz, pyridine); ^{13}C NMR (DMSO-d_6, 62.9 MHz) δ 25.4, 27.5, 27.9, 28.4, 59.3, 59.8, 64.3, 68.2, 69.20, 101.9, 107.2, 111.3, 115.4, 121.7, 123.8, 126.8, 127.6, 128.6, 144.2, 144.51, 151.24, 157.2, 162.60, 163.46, 176.7. Anal. Calcd for $C_{26}H_{26}NO_3$ (400.50): C, 77.97; H, 6.54; N, 3.50. Found: C, 78.12; H, 6.62; N, 3.88.

4.1.5.16. 1-(4-((2-(4-Chlorophenyl)-4-oxo-4H-chromen-7-yl)oxy)butyl)-4-ethylpyridin-1-ium ***(18)***. Yield 82%; off Brown solid; mp 122–123 °C; IR (KBr, cm^{-1}) υ_{max}: 3032 (C—H aromatic), 2955 (C—H), 1627 (C═O), 1117 (C—O). ^{1}H NMR (DMSO-d_6, 250 MHz) δ 1.22 (t, 3H, J = 7 Hz, CH_3), 1.76 (bs, 2H, CH_2), 2.07 (bs, 2H, CH_2), 2.86 (d, 2H, J = 7 Hz, CH_3—C$\underline{H}_2$), 4.15 (bs, 2H, O—CH_2), 4.62 (bs, 2H, N-CH_2), 6.97 (bs, 2H, $H_{3,6}$), 7.28 (d, 2H, J = 2.0 Hz, $H_{1',5'}$), 7.62 (bs, 2H, $H_{2',4'}$), 7.88–8.09 (m, 3H, H_8 and pyridine), 8.41 (bs, 1H, H_5), 9.00 (d, 2H, J = 6.0 Hz, pyridine); ^{13}C NMR (DMSO-d_6, 62.9 MHz) δ 13.8, 25.4, 28.4, 59.9, 68.2, 101.9, 107.5, 115.5, 123.9, 126.6, 127.7, 128.4, 129.6, 130.4, 136.9, 144.5, 149.5, 157.8, 161.4, 16.51, 176.7. Anal. Calcd for: $C_{26}H_{25}ClNO_3$ (434.94): C, 71.80; H, 5.79; N, 3.22. Found: C, 71.42; H, 6.09; N, 3.18.

4.1.5.17. 4-Ethyl-1-(4-((2-(4-methoxyphenyl)-4-oxo-4H-chromen-7-yl) oxy)butyl)pyridin-1-ium ***(19)***. Yield 85%; Brown liquid; IR (KBr, cm^{-1}) υ_{max}: 3045 (C—H aromatics), 2934 (C—H), 1627(C═O), 1179.11 (C—O). ^{1}H NMR (DMSO-d_6, 250 MHz) δ 1.22 (t, 3H, J = 7.5 Hz, CH_3), 1.77–2.04 (m, 4H, CH_2), 2.56 (m, 2H, CH_3—C$\underline{H}_2$), 3.81 (s, 3H, OCH_3), 4.14 (bs, 2H, O—CH_2), 4.64 (bs, 2H, N-CH_2), 6.82 (s, 1H, H_3), 6.97–7.25 (m, 3H, $H_{6,2',4'}$), 7.87–8.02 (m, 2H, $H_{8,1',5'}$), 7.90 (m, 3H, H_5 and pyridine), 9.01 (d, 2H, J = 5 Hz, pyridine); ^{13}C NMR (DMSO-d_6, 62.9 MHz) δ 14.6, 25.4, 27.7, 55.9, 59.9, 68.1, 101.8, 105.6, 114.9, 115.2, 117.5, 123.8, 126.5, 127.6, 128.4, 144.4, 149.8, 153.0, 157.7, 162.4, 163.3, 164.2, 176.7. Anal. Calcd for: $C_{27}H_{28}NO_4$ (430.52): C, 75.33; H, 6.56; N, 3.25. Found: C, 75.61; H, 6.45; N, 3.08.

4.1.5.18. 1-(5-((4-Oxo-4H-chromen-7-yl) oxy) pentyl) pyridin-1-ium ***(20)***. White solid; yield 95%; mp 95–96 °C; IR (KBr, cm^{-1}) υ_{max}: 3051 (C—H aromatic), 2864–2934 (C—H), 1644 (C═O), 1077 (C—O); ^{1}H NMR (DMSO-d_6, 500 MHz,) δ 1.42–1.48 (m, 2H, CH_2), 1.78–1.82 (m, 2H, CH_2), 1.83–1.20 (m, 2H, CH_2), 4.11 (t, 2H, J = 6.5 Hz, O—CH_2), 4.66 (t, 2H, J = 8.5 Hz, N—CH_2), 6.26 (d, 1H, J = 8.5 Hz, H_3), 7.01 (d , 1H, J = 9.0 Hz, H_6), 7.10 (s, 1H, H_8), 7.92 (d, 1H, J = 8.5 Hz, H_5), 8.18 (t, 2H, J = 6.5 Hz, pyridine), 8.22 (d, 1H, J = 7.5 Hz, H_2), 8.62 (t, 1H, J = 8.0 Hz, pyridine), 9.14 (d, 2H, J = 6.0 Hz, pyridine); ^{13}C NMR (DMSO-d_6, 125 MHz) δ 21.9, 27.7, 30.3, 60.5, 68.0, 101.2, 112.1, 114.9, 118.0, 126.4, 128.1, 144.7, 145.5, 156.5, 157.7, 163.0, 175.7. Anal. Calcd for $C_{19}H_{20}NO_3$ (310.37): C, 73.53; H, 6.50; N, 4.51. Found: C, 73.68; H, 6.60; N, 4.43.

4.1.5.19. 1-(5-((4-Oxo-2-phenyl-4H-chromen-7-yl) oxy) pentyl) pyridin-1-ium ***(21)***. Brown solid; yield 87%; mp 145–146 °C; IR (KBr, cm^{-1}) υ_{max}: 3052 (C—H aromatic), 2947 (C—H), 1633 (C═O), 1013 (C—O); ^{1}H NMR (DMSO-d_6, 500 MHz) δ 1.45 (bs, 2H, CH_2), 1.82 (bs, 2H, CH_2), 2.01 (bs, 2H, CH_2), 4.13 (bs, 2H, O—CH_2), 4.67 (bs, 2H, N—CH_2), 6.97 (s, 1H, H_3), 7.02 (bs, 1H, H_6), 7.31 (s, 1H, H_8), 7.59 (bs, 3H, $H_{2',3',4'}$), 7.77 (bs, 2H, $H_{1',5'}$), 7.92 (bs, 1H, H_5), 8.08 (bs, 2H, pyridine), 8.62 (bs, 1H, pyridine), 9.17 (bs, 2H, pyridine); ^{13}C NMR (DMSO-d_6, 125 MHz) δ 21.9, 27.7, 30.3, 60.5, 68.1, 101.3, 106.7, 115.0, 117.0, 123.9, 126.2, 128.1, 129.1, 131.1, 144.7, 145.5, 157.5, 162.1, 163.1, 176.4. Anal. Calcd for $C_{25}H_{24}NO_3$ (386.47): C, 77.70; H, 6.26; N, 3.62. Found: C, 77.45; H, 6.38; N, 3.78.

4.1.5.20. 1-(5-((2-(4-Chlorophenyl)-4-oxo-4H-chromen-7-yl) oxy) pentyl) pyridin-1-ium ***(22)***. Pink solid; yield 96%; mp 94–95 °C; IR (KBr, cm^{-1}) υ_{max}: 3055 (C—H aromatic), 2865–2937 (C—H), 1637 (C═O), 1008 (C—O); ^{1}H NMR (DMSO-d_6, 500 MHz) δ 1.45 (t, 2H, J = 6.5 Hz, CH_2), 1.81 (t, 2H, J = 6.5 Hz, CH_2), 2.01 (bs, 2H, CH_2), 4.11 (t, 2H, J = 6.0 Hz, O—CH_2), 4.69 (bs, 2H, N—CH_2), 6.95 (s, 1H, H_3), 7.00 (d, 1H, J = 8.8 Hz, H_6), 7.27 (s,1H, H_8), 7.61 (d, 2H, J = 8.5 Hz, $H_{1',5'}$), 7.89 (d, 1H, J = 10.0 Hz, H_5), 8.08 (d, 2H, J = 8.5 Hz, $H_{2',4'}$), 8.18 (t, 2H, J = 6.0 Hz, pyridine), 8.62 (t, 1H, J = 7.5 Hz, pyridine), 9.20 (t, 2H, J = 5.5 Hz, pyridine); ^{13}C NMR (DMSO-d_6, 125 MHz) δ 22.0, 27.7, 29.9, 60.1, 68.2, 101.4, 107.0, 115.1, 117.0, 126.2, 128.0, 128.1, 129.2, 130.0, 144.8, 145.5, 157.4, 160.9, 163.2, 176.4. Anal. Calcd for $C_{25}H_{23}ClNO_3$ (420.91): C, 71.34; H, 5.51; N, 3.33. Found: C, 71.18; H, 5.15; N, 3.23.

4.1.5.21. 1-(5-((2-(4-Methoxyphenyl)-4-oxo-4H-chromen-7-yl) oxy) pentyl) pyridin-1-ium ***(23)***. Yellow solid; yield 91%; mp 170–172 °C; IR (KBr, cm^{-1}) υ_{max}: 3049 (C—H aromatic), 2872–2945 (C—H), 1625 (C═O), 1026 (C—O); ^{1}H NMR (DMSO-d_6, 500 MHz) δ 1.45 (bs, 2H, CH_2), 1.8 (bs, 2H, CH_2), 2.02 (bs, 2H, CH_2), 3.83 (s, 3H, OCH_3), 4.12 (t, 2H, J = 7.0 Hz, O—CH_2), 4.69 (t, 2H, J = 8.5 Hz, N—CH_2), 6.83 (s, 1H, H_3), 6.99 (d,1H, J = 10.0 Hz, H_6), 7.09 (d, 2H, J = 8.5 Hz, $H_{2',4'}$), 7.26 (s, 1H, H_8), 7.89 (d, 1H, J = 10.0 Hz, H_5), 8.01 (d, 2H, J = 13.0 Hz, $H_{1',5'}$), 8.18 (t, 2H, J = 6.5 Hz, pyridine), 8.62 (t,1H, J = 9.0 Hz, pyridine), 9.19 (t, 2H, J = 6.0 Hz, pyridine); ^{13}C NMR (DMSO-d_6, 125 MHz) δ 22.0, 27.7, 30.4, 55.6, 60.1, 60.5, 101.3, 105.2, 114.8, 117.0, 123.2, 123.9, 126.1, 128.0, 144.8, 145.5, 157.3, 162.2, 163.0, 176.3. Anal. Calcd for $C_{26}H_{26}NO_4$ (416.50): C, 74.98; H, 6.29; N, 3.36. Found: C, 74.86; H, 6.41; N, 3.28.

4.1.5.22. 4-Ethyl-1-(5-((4-oxo-2-phenyl-4H-chromen-7-yl) oxy) pentyl) pyridin-1-ium ***(24)***. Yield 78%; off yellow solid; mp 137–139 °C; IR (KBr, cm^{-1}) υ_{max}: 3047 (C—H aromatic), 2870–2944 (C—H), 1629 (C═O), 1171 (C—O). ^{1}H NMR (DMSO-d_6, 250 MHz) δ 1.10 (t, 3H, CH_3), 1.40 (bs, 2H, CH_2), 1.80–2.00 (m, 4H, CH_2), 2.87 (q, 2H, J = 7.5 Hz, CH_3—C$\underline{H}_2$), 4.12 (t, 2H, J = 6.0 Hz, O—CH_2), 4.58 (t, 2H, J = 7.5 Hz, N-CH_2), 6.95 (s, 1H, H_3), 7.02 (d, 1H, J = 9.2 Hz, H_6), 7.28 (s, 1H, H_8), 7.55–7.57 (m, 3H, $H_{2',3',4'}$), 7.90–8.06 (m, 5H, $H_{1',5',5}$ and pyridine), δ: 8.99 (d, 2H, J = 6.0 Hz, pyridine); ^{13}C NMR (DMSO-d_6, 62.9 MHz) δ 13.8, 22.4, 28.1, 28.42, 30.6, 60.1, 68.5, 101.8, 107.2, 115.4, 117.5, 126.6, 127.6, 129.5, 131.60 132.1, 144.5, 157.9, 162.5, 164.1, 176.8. Anal. Calcd for $C_{27}H_{28}NO_3$ (414.52): C, 78.23; H, 6.81; N, 3.38. Found: C, 78.42; H, 7.03; N, 3.11.

4.1.5.23. 1-(5-((2-(4-Chlorophenyl)-4-oxo-4H-chromen-7-yl)oxy)pentyl)-4-ethylpyridin-1-ium ***(25)***. Yield 90%; Brown solid; mp 123–124 °C; IR (KBr, cm^{-1}) υ_{max}: 3045 (C—H aromatic), 2865–2930 (C—H), 1642 (C═O), 1176 (C—O). ^{1}H NMR (DMSO-d_6, 250 MHz) δ 1.20 (t, 3H, J = 7.5 Hz, CH_3), 1.42 (bs, 2H, CH_2), 1.77–1.96 (m, 4H, CH_2), 2.87 (q, 2H, J = 7.5 Hz, CH_3—C$\underline{H}_2$), 4.09 (bs, 2H, O—CH_2), 4.58 (bs, 2H, N—CH_2), 6.92–6.98 (m, 2H, $H_{3,6}$), 7.23 (s, 1H, H_8), 7.57 (d, 2H, J = 7.5 Hz, $H_{1',5'}$), 7.83–8.02 (m, 6H, $H_{5,8,2',4'}$ and pyridine), 9.02 (bs, 2H, pyridine); ^{13}C NMR (DMSO-d_6, 62.9 MHz) δ 13.8, 22.3, 28.1, 28.4, 30.6, 60.1, 68.5, 101.7, 107.4, 115.5, 117.4, 126.5, 127.6, 128.4, 129.5, 130.4, 136.8, 144.4, 157.8, 161.3, 163.6, 164.1, 176.7. Anal. Calcd for $C_{27}H_{27}ClNO_3$ (448.97): C, 72.23; H, 6.06; N, 3.12. Found: C, 72.48; H, 5.86; N, 3.48.

4.1.5.24. 4-Ethyl-1-(5-((2-(4-methoxyphenyl)-4-oxo-4H-chromen-7-yl) oxy)pentyl)pyridin-1-ium ***(26)***. Yield 92%; Brown liquid; IR (KBr, cm^{-1}) υ_{max}: 3035 (C—H aromatic), 2939 (C—H), 1628 (C═O), 1177 (C—O). ^{1}H NMR (DMSO-d_6, 250 MHz) δ 1.22 (t, 3H, J = 7.5 Hz, CH_3), 1.42 (bs, 2H, CH_2), 1.78–1.97 (m, 4H, CH_2), 2.87 (q, 2H, J = 7.5 Hz, CH_3—C$\underline{H}_2$), 3.40 (s, 3H, OCH_3), 4.08 (bs, 2H, O—CH_2), 4.60 (bs, 2H, N—CH_2), 6.79 (s, 1H, H_3), 6.93–7.07 (m, 3H, $H_{6,2',4'}$), 7.21 (s, 1H, H_8), 7.83–8.08 (m, 5H, $H_{5,1',5'}$ and pyridine), 9.04 (d, 2H, J = 6.0 Hz, pyridine); ^{13}C NMR (DMSO-d_6, 62.9 MHz) δ 13.8, 22.4, 28.1, 28.4, 30.7, 56.0, 60.1, 68.5, 101.7, 105.6, 114.9, 115.1, 126.5, 127.6, 128.4, 144.5, 149.8, 162.6, 163.4, 164.1, 178.9. Anal. Calcd for: $C_{28}H_{30}NO_4$ (444.55): C, 75.65; H,

6.80; N, 3.15. Found: C, 75.14; H, 5.92; N, 3.35.

4.2. Biological assays

4.2.1. In vitro AChE/BuChE inhibition assay

The method of Ellman et al. was used to determine the inhibitory activity of the compounds against ChEs [51]. All compounds were dissolved in DMSO and the stock solution was prepared at 4.3 mM concentration. The serial dilution was used to obtain 4 test solutions. At first, the compounds were tested at 100 μM in well concentration. If the percent of inhibition was greater than 50%, the assay was performed at 10, 1, 0.1, 0.01 and 0.001 μM for each compound. Briefly, in each well phosphate buffer (2 mL, pH = 8.0) was added followed by adding 20 μL of the AChE or BuChE (2.5 IU/mL), 50 μL of inhibitor and 60 μL of 5,5́-dithio-bis(2-nitrobenzoic acid) (DTNB). The as-prepared cocktail was incubated for 15 min, 20 μL of substrate (acetylthiocholine iodide or butyrylthiocholine iodide) was then added and the absorbance was measured at 412 nM using Biotek Synergy HT microplate reader. Microsoft Excel 2016 was used for calculation of IC_{50}s. Each experiment was repeated at least three independent times and each assay was run in triplicate.

4.2.2. Determination of the inhibitory potency of the compounds against self-induced and AChE-induced $A\beta_{1\text{-}42}$ aggregation

The self- and AChE-induced $A\beta_{1\text{-}42}$ aggregation was performed based on ThT fluorometric assay [52,53]. Aβ sample (Bachem company, Switzerland) was treated with 1,1,1,3,3,3-hexafluoro-2-propanol (HFIP) and diluted in assay sodium phosphate buffer (0.215 M, pH 8) to make a stock solution (50 μM). The peptide was incubated in phosphate buffer (pH 7.4) at 37 °C for 48 h with or without inhibitor (final Aβ concentration was 25 μM). The inhibitor was dissolved in DMSO and diluted in the assay buffer at a final concentration of 10 μM. For co-incubation experiments, the mixtures with a volume of 20 μL, including $A\beta_{1\text{-}42}$ peptide and AChE (Sigma, Electrophorus electricus) in presence or absence of the test inhibitor were incubated for 24 h at room temperature. The final concentrations of $A\beta_{1\text{-}42}$ peptide, AChE and the samples were 200 μM, 2 μM and 100 μM in assay buffer, respectively. After incubation, samples were diluted with 180 μL of ThT (5 mM in 50 mM glycine-NaOH buffer, pH = 8.5) to a final volume of 200 μL. Blank containing Aβ/AChE plus inhibitor and ThT was used in the experiment. The fluorescence intensity was measured (at λ_{ex} = 446 nm; λ_{em} = 490 nm) with multi-mode plate reader (EnSpire, PerkinElmer Waltham, Massachusetts, United States), each reaction was repeated at least three independent times and each assay was run in triplicate. The percentage of inhibition was calculated by the following equation: 100 - [(IF_i - IF_b)/(IF_o - IF_b) − 100], which IF_i, IF_o and IF_b are the fluorescence intensities for Aβ ± AChE aggregation in the presence of inhibitors, in the absence of inhibitors and the blanks, respectively.

4.2.3. Neuroprotection assay against H_2O_2-induced cell death in PC12 cells

The cell viability was determined with the MTT [3-(4,5-dimethylthiazol-2-yl)-2,5-diphenyl tetrazolium bromide] assay [54]. PC12 cells (from the Iranian Biological Resource Center, IBRC) were seeded at 1×10^4 cells/well. Cells were incubated at 37 °C under 5% CO_2 atmosphere for 24 h, then treated with the tested compound (0.1–50 μM) and incubated for 3 h. After that, the cells were exposed to H_2O_2·(150 μM) for 2 h again. MTT solution (20 μL, 5 mg/mL) was next replaced with the medium and incubated for 4 h. The formazan crystals were dissolved with DMSO (100 μL) and the assay was performed by a multi-mode plate reader (Biotek, Winooski, VT) at 570 nm.

4.2.4. Neuroprotection assay against $A\beta_{1\text{-}42}$-induced cytotoxicity in PC12 cells

MTT assay was used to determined cell viability of rat pheochromocytoma PC12 cells (from the American Type Culture Collection, ATCC, Manassas, VA, USA) [55]. The cells were maintained in RPMI-1640 media containing heat-inactivated FBS (10%) and penicillin–streptomycin (1%) and incubated at 37 °C under 5% CO_2 atmosphere and treated with the tested compound (0.01–100 μM) and incubated for 3 h. After that, the cells were exposed to $A\beta_{1\text{–}42}$ (25 μM). After 24 h of incubation, MTT solution (5 mg/mL) was added and the formazan crystals were dissolved with DMSO. The assay was performed by a micro plate reader (Model 680; Bio-Rad Laboratories, Hercules, CA, USA) at 570 nm.

4.2.5. Determination of cytotoxicity effect

Two cancer cell lines of PC12 (rat pheochromocytoma) and HepG2 (human hepatocarcinoma) as well as normal cell of human dermal fibroblast (HDF) were provided by the IBRC cell bank (Tehran, Iran) and cultured in appropriate medium (RPMI-1640 fortified by 10% FBS) using a CO_2 incubator at 37 °C. At the exponential phase of growth, an amount of 10,000 cells were harvested and separately inserted into each well of a 96-well microplate and incubated for 24 h to adhere the cells. Compounds **10** or **14** in the desired concentration range (0–750 μM) and donepezil in corresponding concentrations (0–500 μM) was added to the related wells and the wells were incubated for further 24 h. The media was subsequently removed from each well and MTT solution (5 mg/mL dissolved in RPMI-1640 medium) was added to each well and the well was incubated for 4 h followed by replacing the media with DMSO (100 μL) to dissolve the formed formazan crystals and reading the absorbance at 570 nm and calculating the viability percent and IC_{50} of each compound.

4.2.6. Docking simulations

For docking study, the structure of the compounds was sketched by Chemdraw 19. The smiles were copied to MOE 2019.0102 and prepared by Quickprep module. 1EVE PDB code of AChE and 4BDS code for BuChE were used as enzyme templates for docking due to the high resolution of these codes.

The active site was constructed using Site-Finder module. Rigid body docking was run using default parameters of Autodock Vina program [56]. The best pose of the docking was chosen for ligand-enzyme interaction study by Discovery Studio Modeling [57].

Declaration of Competing Interest

The authors declare that they have no known competing financial interests or personal relationships that could have appeared to influence the work reported in this paper.

Acknowledgments

This work was supported by a grant from National Institute for Medical Research Development (NIMAD; grant number: 983662).

Appendix A. Supplementary material

Supplementary data to this article can be found online at https://doi.org/10.1016/j.bioorg.2021.104750.

References

[1] D.H. Small, R. Cappai, Alois Alzheimer and Alzheimer's disease: a centennial perspective, J. Neurochem. 99 (2006) 708–710.
[2] P. Sharma, P. Srivastava, A. Seth, P.N. Tripathi, A.G. Banerjee, S.K. Shrivastava, Comprehensive review of mechanisms of pathogenesis involved in Alzheimer's disease and potential therapeutic strategies, Prog. Neurobiol. 174 (2019) 53–89.
[3] M. Mehta, A. Adem, M. Sabbagh, New acetylcholinesterase inhibitors for Alzheimer's disease, Int. J. Alzheimers Dis. 2012 (2012) 1–8.
[4] S.N. Dighe, G.S. Deora, E.D. Mora, F. Nachon, S. Chan, M. Parat, X. Brazzolotto, B. P. Ross, Discovery and structure−activity relationships of a highly selective butyrylcholinesterase inhibitor by structure-based virtual screening, J. Med. Chem. 59 (2016) 7683–7689.

[5] T. Arendt, V. Bigl, F. Walther, M. Sonntag, Decreased ratio of CSF acetylcholinesterase to butyrylcholinesterase activity in Alzheimer's disease, Lancet. 323 (1984) 173.

[6] Q. Li, H.Y. Yang, Y. Chen, H.P. Sun, Recent progress in the identification of selective butyrylcholinesterase inhibitors for Alzheimer's disease, Eur. J. Med. Chem. 132 (2017) 294–309.

[7] M.M. Mesulam, A. Guillozet, P. Shaw, A. Levey, E.G. Duysen, O. Lockridge, Acetylcholinesterase knockouts establish central cholinergic pathways and can use butyrylcholinesterase to hydrolyze acetylcholine, Neuroscience. 110 (2002) 627–639.

[8] a) N.H. Greig, T. Utsuki, D.K. Ingram, Y. Wang, G. Pepeu, C. Scali, Q. Yu, J. Mamczarz, H.W. Holloway, T. Giordano, et al., Selective butyrylcholinesterase inhibition elevates brain acetylcholine, augments learning and lowers Alzheimer β-amyloid peptide in rodent, Proc. Natl. Acad. Sci. USA 102 (2005) 17213–17218; b) E. Giacobini, Selective inhibitors of butyrylcholinesterase: a valid alternative for therapy of Alzheimer's disease? Drugs Aging 18 (2001) 891–898.

[9] X.u. Han, G. He, Toward a rational design to regulate β-amyloid fibrillation for Alzheimer's disease treatment, ACS Chem. Neurosci. 9 (2) (2018) 198–210.

[10] N.N. Nalivaeva, A.J. Turner, AChE and the amyloid precursor protein (APP)–Cross-talk in Alzheimer's disease, Chem. Biol. Interact. 259 (2016) 301–306.

[11] a) N.C. Inestrosa, J.P. Sagal, M. Colombres, Acetylcholinesterase interaction with Alzheimer amyloid beta, Subcell Biochem. 38 (2005) 299–317; b) A. Castro, A. Martı'nez, Peripheral and dual binding site acetylcholinesterase inhibitors: implications in treatment of Alzheimer's disease, Mini-Rev. Med. Chem. 3 (2001) 267–272.

[12] Yu Wang, Hao Wang, Hong-zhuan Chen, AChE inhibition-based multi-target-directed ligands, a novel pharmacological approach for the symptomatic and disease-modifying therapy of Alzheimer's disease, Curr. Neuropharmacol. 14 (4) (2016) 364–375.

[13] S. Diamant, E. Podoly, A. Friedler, H. Ligumsky, O. Livnah, H. Soreq, Butyrylcholinesterase attenuates amyloid fibril formation in vitro, Proc. Natl. Acad. Sci. USA 103 (23) (2006) 8628–8633.

[14] Erez Podoly, Geula Hanin, Hermona Soreq, Alanine-to-threonine substitutions and amyloid diseases: Butyrylcholinesterase as a case study, Chem. Biol. Interact. 187 (1-3) (2010) 64–71.

[15] Sultan Darvesh, Meghan K. Cash, George Andrew Reid, Earl Martin, Arnold Mitnitski, Changiz Geula, Butyrylcholinesterase is associated with β-amyloid plaques in the transgenic APP SWE/PSEN1dE9 mouse model of alzheimer disease, J. Neuropathol. 71 (1) (2012) 2–14.

[16] C.S. Atwood, M.E. Obrenovich, T. Liu, et al., Amyloid-β: a chameleon walking in two worlds: a review of the trophic and toxic properties of amyloid-β, Brain Res. Rev. 43 (2003) 1–16.

[17] C. Behl, J.B. Davis, R. Lesley, D. Schubert, Hydrogen peroxide mediates amyloid beta protein toxicity, Cell. 77 (1994) 817–827.

[18] Brian J. Tabner, Omar M.A. El-Agnaf, Stuart Turnbull, Matthew J. German, Katerina E. Paleologou, Yoshihito Hayashi, Leanne J. Cooper, Nigel J. Fullwood, David Allsop, Hydrogen peroxide is generated during the very early stages of aggregation of the amyloid peptides implicated in Alzheimer disease and familial British dementia, J. Biol. Chem. 280 (43) (2005) 35789–35792.

[19] Xiao-Lan Qi, Jin Xiu, Ke-Ren Shan, Yan Xiao, Ran Gu, Ru-Yu Liu, Zhi-Zhong Guan, Oxidative stress induced by beta-amyloid peptide1-42 is involved in the altered composition of cellular membrane lipids and the decreased expression of nicotinic receptors in human SH-SY5Y neuroblastoma cells, Neurochem. Int. 46 (8) (2005) 613–621.

[20] K. Rajasekhar, Malabika Chakrabarti, T. Govindaraju, Function and toxicity of amyloid beta and recent therapeutic interventions targeting amyloid beta in Alzheimer's disease, Chem. Commun. 51 (70) (2015) 13434–13450.

[21] María Jesús Oset-Gasque, José Marco-Contelles, Alzheimer's disease, the "one-molecule, one-target" paradigm, and the multitarget directed ligand approach, ACS Chem. Neurosci. 9 (3) (2018) 401–403.

[22] M.J. Mphahlele, E.N. Agbo, S. Gildenhuys, I.B. Setshedi, Exploring biological activity of 4-oxo-4H-furo[2,3-h]chromene derivatives as potential multi-target-directed ligands inhibiting cholinesterases, β-secretase, cyclooxygenase-2, and lipoxygenase-5/15, Biomolecules 9 (2019) 736–760.

[23] J. Jończyk, K. Lodarski, M. Staszewski, J. Godyń, P. Zaręba, O. Soukup, J. Janockova, J. Korabecny, K. Salat, N. Malikowska-Racia, M. Hebda, N. Szalaj, B. Filipek, K. Walczyński, B. Malawska, M. Bajda, Search for multifunctional agents against Alzheimer's disease among non-imidazole histamine H3 receptor ligands. *In vitro* and *in vivo* pharmacological evaluation and computational studies of piperazine derivatives, Bioorg. Chem. 90 (2019), 103084.

[24] Richard Morphy, Zoran Rankovic, Fragments, network biology and designing multiple ligands, Drug Discov. Today 12 (3-4) (2007) 156–160.

[25] C.F.M. Silva, D.C.G.A. Pinto, A.M.S. Silva, Chromones: privileged scaffolds for the production of multi-target-directed-ligand agents for the treatment of Alzheimer's disease, Expert. Opin. Drug Discov. 13 (2018) 1141–1151.

[26] B.C. Adedayo, G. Oboh, S. Oyeleye, I.I. Ejakpovi, A.A. Boligon, M.L. Athayde, Blanching alters the phenolic constituents and in vitro antioxidant and anticholinesterases properties of fireweed (Crassocephalum crepidioides), J. Taibah Uni. Med. Sci. 10 (2015) 419–426.

[27] I. Uriarte-Pueyo, M.I. Calvo, Flavonoids as acetylcholinesterase inhibitors, Curr. Med. Chem. 18 (2011) 5289–5302.

[28] H. Kim, B.S. Park, K.G. Lee, C.Y. Choi, S.S. Jang, Y.H. Kim, S.E. Lee, Effects of naturally occurring compounds on fibril formation and oxidative stress of beta-amyloid, J. Agric. Food Chem. 53 (2005) 8537–8541.

[29] A. Iida, T. Usui, F. Zar Kalai, J. Han, H. Isoda, Y. Nagumo, Protective effects of Nitraria retusa extract and its constituent isorhamnetin against amyloid binduced cytotoxicity and amyloid b aggregation, Biosci. Biotechnol. Biochem. 79 (2015) 1548–1551.

[30] David Vauzour, Katerina Vafeiadou, Ana Rodriguez-Mateos, Catarina Rendeiro, Jeremy P.E. Spencer, The neuroprotective potential of flavonoids: a multiplicity of effects, Gene. Nutr. 3 (3-4) (2008) 115–126.

[31] Seyed Fazel Nabavi, Nady Braidy, Solomon Habtemariam, Ilkay Erdogan Orhan, Maria Daglia, Azadeh Manayi, Olga Gortzi, Seyed Mohammad Nabavi, Neuroprotective effects of chrysin: from chemistry to medicine, Neurochem. Int. 90 (2015) 224–231.

[32] J.K. Li, Z.T. Jiang, R. Li, Investigation of antioxidant activities and free radical scavenging of flavonoids in leaves of Polygonum multiflorum Thumb, China Food Addit. 2 (2012) 69–74.

[33] S. Kumar, A. Mishra, A.K. Pandey, Antioxidant mediated protective effect of Parthenium hysterophorus against oxidative damage using in vitro models, BMC Compl. Altern. Med. 13 (2013) 120.

[34] Monica Leopoldini, Nino Russo, Sandro Chiodo, Marirosa Toscano, Iron chelation by the powerful antioxidant flavonoid quercetin, J. Agric. Food Chem. 54 (17) (2006) 6343–6351.

[35] R. Gautam, S.M. Jachak, V. Kumar, C.G. Mohan, Synthesis, biological evaluation and molecular docking studies of stellatin derivatives a cyclooxygenase (COX-1, COX-2) inhibitors and anti-inflammatory agents, Bioorg. Med. Chem. 21 (2011) 1612–1616.

[36] (a) C.X. Gong, F. Liu, K. Iqbal, Multifactorial hypothesis and multi-targets for Alzheimer's disease, J. Alzheimers Dis. 64 (2018) S107–S117; (b) J. Reis, A. Gaspar, N. Milhazes, F. Borges, Chromone as a privileged scaffold in drug discovery: recent advances, J. Med Chem. 60 (2017) 7941–7957; (c) L. Jalili- Baleh, E. Babaei, Sh. Abdpour, S.N.A. Bukhari, A. Foroumadi, A. Ramazani, M. Sharifzadeh, M. Abdollahi, M. Khoobi, A review on flavonoid-based scaffolds as multi-target-directed ligands (MTDLs) for Alzheimer's disease, Eur. J. Med. Chem. 152 (2018) 570–589; (d) J. Reis, F. Cagide, M.E. Valencia, J. Teixeira, D. Bagetta, C. Pérez, E. Uriarte, P. J. Oliveira, F. Ortuso, S. Alcaro, M.I. Rodríguez-Franco, F. Borges, Multi-target-directed ligands for Alzheimer's disease: discovery of chromone-based monoamine oxidase/cholinesterase inhibitors, Eur. J. Med. Chem. 158 (2018) 781–800; (e) Z. Sang, K. Wang, J. Shi, W. Liu, X. Cheng, G. Zhu, et al., The development of advanced structural framework as multi-target-directed ligands for the treatment of Alzheimer's disease, Eur. J. Med. Chem. 192 (2020) 112180; (f) S. Chaves, S. Resta, F. Rinaldo, M. Costa, R. Josselin, K. Gwizdala, et al., Design, synthesis, and in vitro evaluation of hydroxybenzimidazole-donepezil analogues as multitarget-directed ligands for the treatment of Alzheimer's disease, Molecules. 25 (2020) 985.

[37] Q. Liu, X. Qiang, Y. Li, Z. Sang, Z.Y. Li, Z. Tan, Y. Deng, Design, synthesis and evaluation of chromone-2-carboxamido-alkylbenzylamines as multifunctional agents for the treatment of Alzheimer's disease, Bioorg. Med. Chem. 23 (2015) 911–923.

[38] L. Jalili-Baleh, H. Nadri, H. Forootanfar, T. TüylüKüçükkılınç, B. Ayazgök, M. Sharifzadeh, M. Rahimifard, M. Baeeri, M. Abdollahi, A. Foroumadi, M. Khoobi, Chromone–lipoic acid conjugate: neuroprotective agent having acceptable butyrylcholinesterase inhibition, antioxidant and copper-chelation activities, DARU J. Pharm. Sci. (2021), https://doi.org/10.1007/s40199-020-00378-1.

[39] a) M. Alipour, M. Khoobi, A. Foroumadi, H. Nadri, A. Moradi, A.h. Sakhteman, M. Ghandi, A. Shafiee, marin derivatives bearing N-benzyl pyridinium moiety: potent and dual binding site acetylcholinesterase inhibitors, Bioorg. Med. Chem. 20 (2012) 7214–7222; b) N. Salehi, B.B.F. Mirjalili, H. Nadri, Z. Abdolahi, H. Forootanfar, A. Samzadeh-Kermani, T.T. Küçükkılınç, B. Ayazgok, S. Emami, I. Haririan, M. Sharifzadeh, A. Foroumadi, M. Khoobi, Synthesis and biological evaluation of new N-benzylpyridinium-based benzoheterocycles as potential anti-Alzheimer's agents, Bioorganic Chemistry, 83 (2019) 559–568. (c) P. Sharma, A. Tripathi, P.N. Tripathi, S.K. Prajapati, A. Seth, M.K. Tripathi, P. Srivastava, V. Tiwari, S. Krishnamurthy, S.K. Shrivastava, Design and development of multitarget-directed N-benzylpiperidine analogs as potential candidates for the treatment of Alzheimer's disease, Eur. J. Med. Chem. 167 (2019) 510–524.

[40] P. Kapkova, V. Alptüzün, P. Frey, E. Erciyas, U. Holzgrabe, Search for dual function inhibitors for Alzheimer's disease: Synthesis and biological activity of acetylcholinesterase inhibitors of pyridinium-type and their Aβ fibril formation inhibition capacity, Bioorg. Med. Chem. 14 (2006) 472–478.

[41] L. Jalili-Baleh, H. Nadri, H. Forootanfar, A. Samzadeh-Kermani, Novel 3-phenyl coumarin-lipoic acid conjugates as multi-functional agents for potential treatment of AD, Bioorg. Chem. 79 (2018) 223–234.

[42] L. Jalili-Baleh, H. Forootanfar, T.T. Küçükkılınç, H. Nadri, Z. Abdolahi, A. Ameri, M. Jafari, B. Ayazgok, M. Baeeri, M. Rahimifard, S.N. Abbas Bukhari, M. Abdollahi, M.R. Ganjaali, S. Emami, M. Khoobi, A. Foroumadi, Design, synthesis and evaluation of novel multi-target-directed ligands for treatment of Alzheimer's disease based on coumarin and lipoic acid scaffolds, Eur. J. Med. Chem. 152 (2018) 600–614.

[43] J.C. Jaen, L.D. Wise, T.G. Heffner, T.A. Pugsley, L.T. Meltzer, Dopamine auto receptor agonists as potential antipsychotics. 2. (Aminoalkoxy)-4H-1-benzopyran-4-ones, J. Med. Chem. 34 (1991) 248–256.

[44] J.H. Kwak, H.E. Kang, J.K. Jung, et al., Synthesis of 7-hydroxy-4-Oxo-4H-chromene and 7-hydroxychroman-2-carboxylic acid N-alkyl amides and their antioxidant activities, Arch. Pharmacal Res. 29 (2006) 728–734.

[45] G. Sagrera, A. Bertucci, A. Vazquez, G. Seoane, Synthesis and antifungal activities of natural and synthetic bioflavonoids, Bioorg. Med. Chem. 19 (2011) 3060–3073.

[46] N.G. Ghodile, P. Rajput, V. Banewar, et al., Synthesis and Antimicrobial activity of some Chalcones and Flavones having 2-hydroxyacetophenone moiety, Int. J. Pharm. Bio Sci. 3 (2012) 389–395.

[47] C.A. Massaad, Neuronal and vascular oxidative stress in Alzheimer's disease, Curr. Neuropharmacol. 9 (2011) 662–673.
[48] SwissADME, a free web tool to evaluate pharmacokinetics, drug-likeness and medicinal chemistry friendliness of small molecules, Sci. Rep. 7 (2017) 42717.
[49] M. Singh, O. Silakari, Design, synthesis and biological evaluation of novel 2-phenyl-1-benzopyran-4-one derivatives as potential poly-functional anti-Alzheimer's agents, RSC Adv. 6 (2016) 108411–108422.
[50] H. Yang, H.J. Zhong, K.H. Leung, et al., Structure-based design of flavone derivatives as c-myc oncogene down-regulators, Eur. J. Pharm. Sci. 48 (2013) 130–141.
[51] G.L. Ellman, K.D. Courtney, V. Andres, R.M. Featherstone, A new and rapid colorimetric determination of acetylcholinesterase activity, Biochem. Pharmacol. 7 (1961) 88–95.
[52] M. Bartolini, C. Bertucci, V. Cavrini, V. Andrisano, b-amiloid aggregation induced by human acetylcholinesterase: inhibition studies, Biochem. Pharmacol. 65 (2003) 407–416.
[53] J. Rouleau, B.I. Iorga, C. Guillou, New potent human acetylcholinesterase inhibitors in the tetracyclic triterpene series with inhibitory potency on amyloid-β aggregation, Eur. J. Med. Chem. 46 (2011) 2193–2205.
[54] D. Zsolt, A. Juhász, M. Gálfi, K. Soós, R. Papp, D. Zádori, B. Penke, Method for measuring neurotoxicity of aggregating polypeptides with the MTT assay on differentiated neuroblastoma, Cells Brain Res. Bull. 62 (2003) 223–229.
[55] H. Levine, Thioflavine T interaction with synthetic Alzheimer's disease beta-amyloid peptide: detection of amyloid aggregation in solution, Protein Sci. 20 (1993) 404–410.
[56] O. Trott, A.J. Olson, AutoDock Vina: improving the speed and accuracy of docking with a new scoring function, efficient optimization and multithreading, J. Comput. Chem. 31 (2010) 455–461.
[57] Dassault Systèmes BIOVIA, Discovery Studio Modeling, Release, 4. San Diego: Dassault Systemes, 2015.